1-1-2008

# An estimation of the performance limits and improvement of dry cooling on trough solar thermal plants

Huifang Deng
*University of Nevada, Las Vegas*

# AN ESTIMATION OF THE PERFORMANCE LIMITS AND IMPROVEMENT OF DRY COOLING ON TROUGH SOLAR THERMAL PLANTS

By

Huifang Deng

Bachelor of Science
University of Science and Technology, Beijing
2008

A thesis submitted in partial fulfillment
of the requirements for the

**Master of Science Degree in Mechanical Engineering**
**Howard R. Hughes College of Engineering**
**Department of Mechanical Engineering**

**Graduate College**
**University of Nevada, Las Vegas**
**August 2008**

UNLV
UNIVERSITY OF NEVADA LAS VEGAS

**Thesis Approval**
The Graduate College
University of Nevada, Las Vegas

July 8, 2008

The Thesis prepared by

Huifang Deng

**Entitled**

An Estimation of the Performance Limits and Improvement of Dry Cooling Trough Solar Thermal Plants

is approved in partial fulfillment of the requirements for the degree of

Master of Science in Mechanical Engineering

*Examination Committee Chair*

*Dean of the Graduate College*

*Examination Committee Member*

*Examination Committee Member*

*Graduate College Faculty Representative*

1017-53

ABSTRACT

**An Estlmation of the Performance Limits and Improvement of Dry Cooling On Trough Solar Thermal Plants**

By

Huifang Deng

Dr. Robert F. Boehm, Examination Committee Chair
Professor of Mechanical Engineering
University of Nevada, Las Vegas

A model of a fairly typical, but simplified, solar trough plant has been developed and simulated to determine its thermodynamic performance using the software GateCycle. The energy generation and cycle efficiency of the plant have been examined for the Las Vegas vicinity with conventional wet cooling and conventional dry cooling cases considered separately using this software. TMY2 data are used for this location for this purpose. Similarly, the same studies are carried out for "ideal" cooling systems as a comparison. It turned out that the ideal dry cooling system would significantly outperform the conventional wet cooling system, indicating the possibility of the dry cooling system being able to achieve increased performance levels with component improvements. Then an advanced circular-tube-circular-fin surface and a flattened-tube surface were applied to the air-cooled condenser and simulated. The results of the new models were compared with that of the default model.

TABLE OF CONTENTS

LIST OF FIGURES

LIST OF TABLES

NOMENCLATURE

| | |
|---|---|
| ACC | Air-cooled condenser |
| $A$ | Tube wall area, $m^2$ |
| $a_c$ $b_c$ | Coefficient for conventional wet cooling systems |
| $a_i$ $b_i$ | Coefficient for ideal wet cooling systems |
| $C$ | Constant depending on tube rows |
| $C_{min}$ | Equals to $C_{air}$ or $C_{steam}$, whichever is smaller, W/ °C |
| $C_p$ | Heat capacity of the air, kJ/kgK |
| $D$ | Diameter of the tube, m |
| DNI | Direct normal incidence, $w/m^2$ |
| $D_o$ | Outer diameter of the tube, m |
| $h_1$ | Steam enthalpy at the turbine inlet, kJ/kg |
| $h_2$ | Steam enthalpy at the turbine outlet, kJ/kg |
| $h_4$ | Steam enthalpy at the boiler inlet, kJ/kg |
| $h_a$ | Convection coefficient of the air side, kJ/kg |
| $h_{fg}$ | Specific enthalpy of evaporation, kJ/kg |
| $h_{fin}$ | Fin height, mm |
| $k$ | Thermal conductivity of the tube wall, W/mK |
| $M_a$ | Mass flow rate of the air, kg/s |

| | |
|---|---|
| $M_s$ | Mass flow rate of the steam, kg/s |
| NTU | Number of Transfer Units |
| $Nu_{air}$ | Nusselt number of the air, dimensionless number |
| $P_1$ | Boiler pressure, kPa |
| $P_3$ | Steam pressure at the pump inlet, kPa |
| $P_{c,1}$ | Condensing pressure in case 1, kPa |
| $P_{c,2}$ | Condensing pressure in case 2, kPa |
| $P_{c,D}$ | Condensing pressure in the default case, kPa |
| Pr | Prandtl number, dimensionless number |
| $P_s$ | Condensing pressure, kPa |
| $Q_{in}$ | Heat provided into the Rankine cycle system, kW |
| q | Real heat transfer rate, kW |
| $q_{max}$ | Maximum heat transfer rate that could exist, kW |
| R | Thermal resistance of the tube wall, °C/W |
| Re | Reynolds number, dimensionless number |
| St | Stanton number, dimensionless number |
| $s_{fin}$ | Fin thickness, mm |
| $T_{a,in}$ | Inlet air temperature of ACC in the design mode, °C |
| $T_{a,out}$ | The air outlet temperature, °C |
| $T_{c,1}$ | Condensing temperature in case 1, °C |
| $T_{c,D}$ | Condensing temperature in the default case, °C |
| $T_{c,2}$ | Condensing temperature in case 2, °C |
| $T_d$ | Ambient dry bulb temperature, °C, °C |

| | |
|---|---|
| $T_{cold,in}$ | The temperature of the cold fluid, °C |
| $T_{hot,in}$ | The temperature of the hot fluid, °C |
| $t_{fin}$ | Fin pitch, mm |
| U | Overall heat transfer coefficient, $W/m^2K$ |
| $V_{air}$ | Face velocity of inlet air, m/s |
| $W_{turbine}$ | Actual work done by the steam turbine, kW |
| $W_p$ | Pump work, kW |
| $X_{inlet}$ | Steam quality at the ACC inlet |
| $X_{outlet}$ | Steam quality at the ACC outlet |
| $\varphi$ | Relative humidity |
| $\eta$ | Rankine cycle efficiency |
| $\eta_{boiler}$ | Boiler efficiency |
| $\eta_{c,1}$ | Rankine cycle efficiency in case 1 |
| $\eta_{c,2}$ | Rankine cycle efficiency in case 2 |
| $\eta_{c,D}$ | Rankine cycle efficiency in the default case |
| $\eta_{d,c}$ | Cycle efficiency of the power plant with the conventional dry cooling system |
| $\eta_{d,i}$ | Cycle efficiency of the power plant with the ideal dry cooling system |
| $\eta_r$ | Receiver efficiency |
| $\eta_{w,c}$ | Cycle efficiency of the power plant with the conventional wet cooling system |

| | |
|---|---|
| $\eta_{w,i}$ | Cycle efficiency of the power plant with the ideal wet cooling system |
| $\gamma$ | Kinematic viscosity, $m^2/s$ |
| $\xi$ | Heat exchange effectiveness, defined as $\xi = q / q_{max}$ |
| $v_m$ | Mean specific volume of the steam, $m^3/kg$ |

## ACKNOWLEDGEMENTS

I would like to express my gratitude to all those who gave me the possibility to complete this thesis.

First of all, I would like to express my appreciation to my first advisor Dr. Tan, Liangcai in UNLV. It was because of his warm invitation and great help that I had the chance to come to UNLV for my Master's study.

I have furthermore to thank my current supervisor Dr. Boehm for offering me the opportunity to commence related research on this topic with free access to all the necessary facilities and data. 'You will be the expert on dry cooling!' I could still remember clearly of his encouraging smile when he ended the first meeting determining my project topic. With his wonderful ideas, profound teaching, the great effort to make our communications more clear and the patient help on my first paper writing once and once again on every aspect, he brought me to a totally new world of research and knowledge and taught me the living principles. I would have been lost without him.

I am also grateful to Ibrahim Mohamed Khalil and Ahmad Abu Heiba for their permission to access their previous work and data, to Mark Campbell, Aaron Sahm and Ahmad Abu Heiba for their valuable help on my research, and to Tasha Ramos for her great carefulness organizing everything at the UNLV solar site, so that we can concentrate on our work.

I am indebted to my dear parents who are always unconditionally supporting me at any time in my life.

I would like to thank all the people working at the solar site for providing a stimulating and fun environment in which to learn and grow.

I wish to thank my roommate Chen, Zhuoqi who has been supporting and accompanying me on all my way to the graduation, also to all other friends who have been sharing all these memories with me.

Finally, I am indebted to the National Renewable Energy Laboratory through the NSWP program for supplying the funding that made this project possible.

# CHAPTER 1

# INTRODUCTION

## Background

The southwestern US is an ideal location for solar power plants due to its abundant solar resource while there is a difficulty in implementing wet cooling systems for Rankine-based systems due to the shortage of water in this region. Dry cooling could be an excellent solution for this, if it could achieve a high efficiency and low condensing temperature as wet cooling.

Actually, as the environmental problems are being viewed with more importance, industries are investing in dry cooling rather than in cheaper wet cooling systems at some locations to conserve water resources (Johnson and Maulbetsch, 1979) (Hintzen and Benzing, 1999). Besides, infinite availability of air as the cooling medium, less pollution, free choice of location, and the simplified approval procedure are also factors that impact the choice of this cooling option (Hintzen and Benzing, 1999).

Although the first use of dry cooling technology was recorded in the 1930s (Kroeger, 1998; Miliaris, 1974), the real history of dry cooling on the substantial units and its evolution began in 1962 with an indirect, natural draft system at Rugeley city in the U.K. (Layton, Matthew S. and O'Hagan, Joseph, 2002). Over the past 40 years, dry cooling technology has experienced great development.

Layton and O'Hagan (2002) showed in their report the increase in the installed MWe of the power plant on the dry cooling technology for both the US and the world; see Figure 1. It is estimated that over 2500 MWe of US power generation and about 15-20 GWe worldwide rely on dry cooling. But it is still a quite small share compared to wet cooling systems.

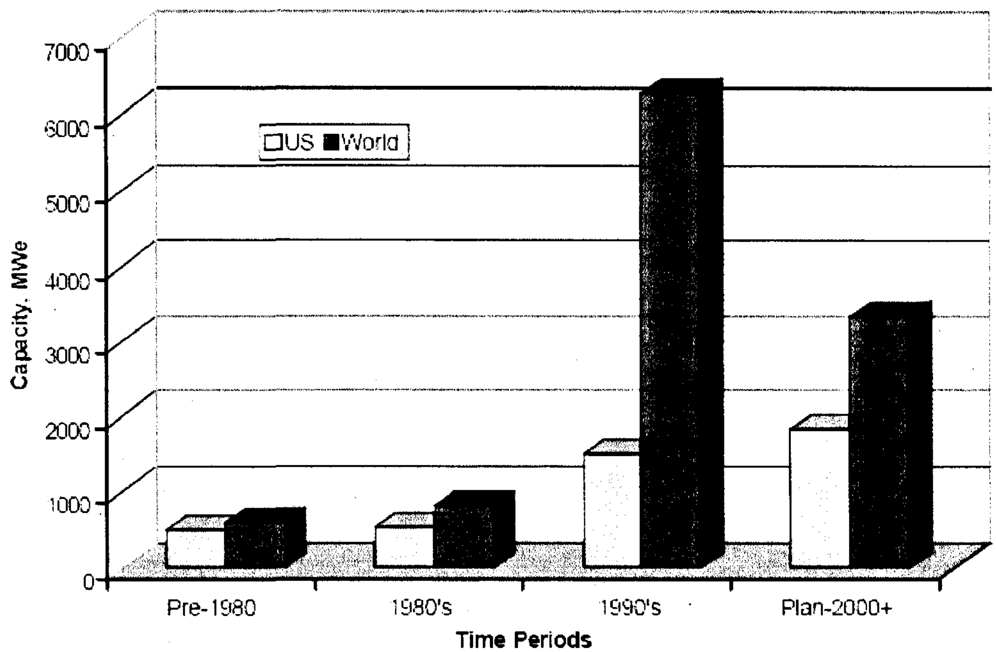


Figure 1 The dry cooling technology development trend [Layton, Matthew S. and O'Hagan, Joseph, 2002]

The report also lists the distribution of U.S. dry cooling units installed and planned by state expressed both as the number of units and as the total generating capacity, see the Appendix. Twenty-three states plus Washington, DC, have some amount of dry cooling, even including many in the Northeast where rainfall and water supply are, at least on average, plentiful. Backer and Wurtz (2003) explained some other possible reasons for the selection. Even if enough water is available, some other factors may play a role as well. At times of high humidity and cool air temperature, a wet cooling tower is likely to produce a plume which is a visible fog exiting the tower. While the plume is environmentally safe – it is nothing but water – it can create visual problems or icing if the plant is located near a highway, residential area or airport.

They also mentioned in their paper that recent studies indicate that on average, one third of the new power plants permitted in North America will require a dry cooling system. This is driven by the lack of water, PM10, and EPA 316(a) and 316 (b) issues. PM10 is one of the seven air pollutants the Environmental Protection Agency (EPA) regulates under the National Ambient Air Quality Standards (NAAQS). PM10 is defined as particulate matter (PM) with a mass median diameter less than 10 micrometers. EPA also regulates the cooling water systems at electric generating plants and manufacturers through sections 316(a) and 316(b) of the Clean Water Act.

As one of the major condensing options, dry cooling technology has earned a significant place in the power generation industry since it emerged several decades ago. A detailed understanding of dry cooling systems is very important in either design or any improvement to them.

Figure 2 shows the structure of a unit in an air-cooled condenser (ACC).

Instead of using cooling water as the wet cooling system does, the air-cooled condenser uses ambient air that is blowing up through the tubes, taking the heat away from the hot steam so that the condensation could occur. The advantages and disadvantages of dry cooling technology are equally obvious due to its structural features.

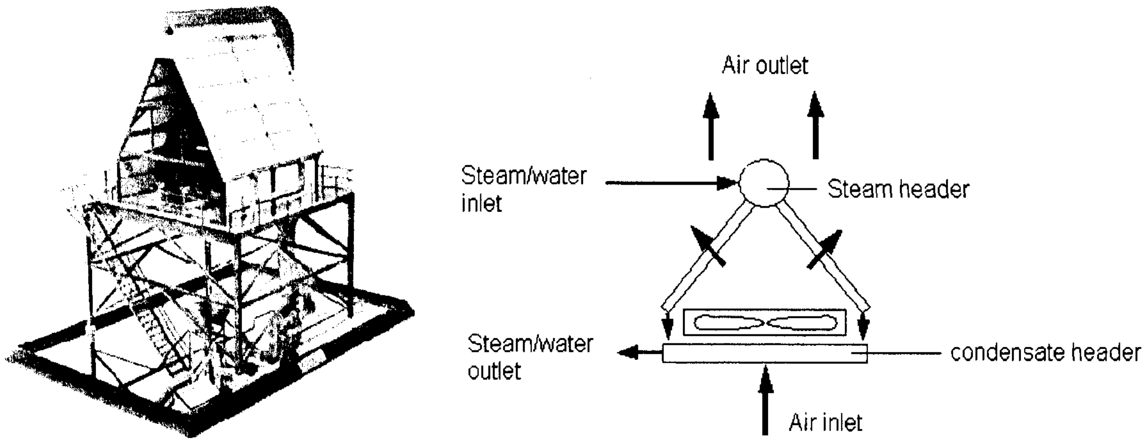


(a) (b)

Figure 2 (a) The structure of a real unit in a dry cooling system (Larinoff M.W., Moles, W.E. and Reichhelm, R. 1978.)
(b) The illustration of the structure of a dry cooling system unit

The steam flows into the main steam header after leaving the steam turbine, and is then distributed into the condensing tubes. As the heat is extracting out by the air, the steam begins to condense once it reaches the saturated temperature. Thus the performance of the air-cooled condenser in a large part depends on the ambient dry bulb temperature, while the performance of wet cooling systems on the ambient wet bulb temperature, in which the heat is rejected through the evaporation process. Since the dry bulb temperature is always higher than the wet bulb temperature, especially in the hot days, the air cooled system performs almost as well as wet cooling systems at low ambient air temperature, but becomes synonymous with lower efficiency and lower plant output when the ambient temperature goes high.

In the recent 40 years, many reports have been made on the efforts to improve the performance of dry cooling systems. As early as the 1970s, an economic optimization option was given by Leung(Leung, 1973) that a dry tower plant would relegate a portion of its generation capability to other plants within the network during summer months. He suggested that its back pressure be limited to approximately 6.0 in. Hg. absolute at reduced load while served by a full-duty heat exchanger to maintain its thermal efficiency, while in winter, operate at 1.0 to 2.0 in. Hg. absolute at maximum load to achieve the best efficiency. With continually escalating fossil-fuel prices at that time, this method of economic optimization would favor a longer last-stage turbine for dry cooling tower applications.

Later a new concept of power plant "heat-sink system" which employed the combination of a conventional wet-tower and a conventional dry-tower to reduce wet cooling-tower makeup-water requirements in water-short areas was considered. In this combination, the dry tower operates all year around while the wet-peaking tower is used only above certain ambient dry-bulb temperatures. (Larinoff and Forster, 1977)

A phase-change dry cooling system that employed ammonia as the heat rejection fluid rather than water was proposed, where high-performance heat exchangers were used to further reduce costs, but the costs of this system remain high with respect to the costs of once-through and evaporative cooling systems (McHale et al., 1979).

Later a concept was proposed which aimed to achieve highest possible thermal efficiency at high temperature by precooling a portion of the air flow with water and causing only this portion to act on the coldest part of the heat exchange surface. (Oplatka, 1981)

Others showed the effectiveness of finned heat-pipes that are ammonia-filled and lined with capillary-wick material applied to dry cooling systems. (Azad and Karimeddini, 1990) From the studies above, we can see that all of the previous investigations have tried to improve performance of existing dry cooling systems by either preprocessing the working fluid or making up the loss with the assistance of other systems. However, work has seldom been reported, to my knowledge, in the detailed study on dry cooling systems themselves.

Many factors or operating parameters affect the performance of dry cooling systems. Among these is the dry bulb temperature which is the major environmental factor that affects the condensing performance of dry cooling systems. The dry bulb temperature changes constantly. For a solar trough power plant with a dry cooling system, weather has a major impact on plant performance. Abundant sunshine in summer could provide more energy for the power plant, but associated high ambient temperatures may decrease the power output of the turbine. Appropriate changes to the heat transfer surface geometry used in air-cooled condensers could result in improved condensing efficiency, which could further lead to a higher Rankine cycle efficiency.

The aim of this thesis is to investigate the influence of these factors on dry cooling systems which in turn affect the power output of the solar plant. Hourly performance and power output are calculated as well. In addition, a comparison with wet cooling systems is conducted.

## GateCycle Software

GE's GateCycle™ (Wyatt Enterprises, LLC. 2007) software is a commercially available, fully flexible heat and mass balance program for Microsoft Windows™. It has been under development since 1981 and is with over 500 users worldwide one of the most widely used software for power plant design and simulation. GateCycle provides a palette of common power plant equipment icons that can be used to construct detailed models of fossil, combined cycle, simple cycle and nuclear power plants, as well as a series of default configuration for each parameter of the equipment that helps users to set up the power plants, shown as Figure 3.

GateCycle is widely used to model the steady state design and off-design performance of thermal power plants. It can perform a large variety of analyses, such as:

1. Designing and analyzing an overall cycle for a proposed power system or cogeneration station.

2. Checking claims made by vendors about the performance of entire power plants or individual hardware.

3. Simulating the performance of existing systems at "off-design" operating conditions.

4. Predicting the effect of proposed changes or enhancements to existing

plants.

5. Analyzing advanced gas turbine designs, including designs that are fully integrated with the steam/water cycle.

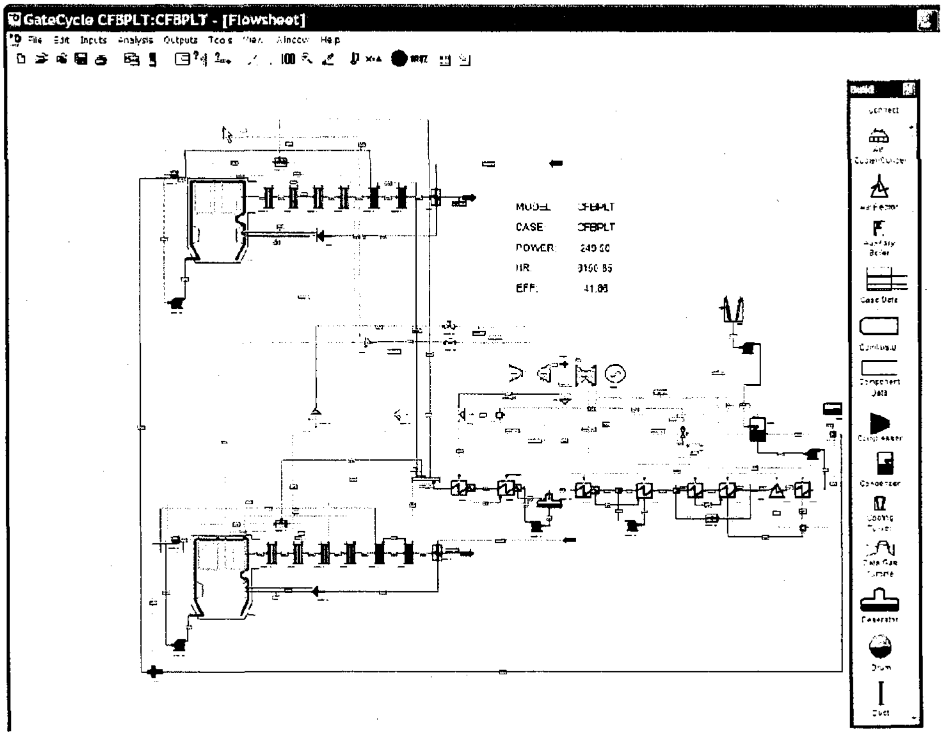


Figure 3 Gatecycle graphical user interface [Wyatt Enterprises, LLC. 2007]

More details could also be found from the official website of GateCycle: http://www.gepower.com/prod_serv/products/oc/en/opt_diagsw/gatecycle.htm.

There are two working modes in GateCycle: design mode and off-design mode. The design-mode run for any GateCycle icon calculates the physical size (and other design parameters) for key specified performance parameter. Once a design case has been created for an equipment icon, this case can be referenced by the same icon running in off-design mode in another case, which enables you to analyze the performance of a “physically-based” equipment icon under off-design operating conditions.

In this study, a simplified Rankine cycle was first configured in the design mode and equipment sized according to some key specifications and certain ambient conditions. Then the performance of the designed Rankine cycle model was simulated under the off-design mode, where the ambient conditions were varied.

# CHAPTER 2

## COMPARISON CHECK OF GATECYCLE

### Methodology

A comparison check was conducted on GateCycle in both the design and the off-design modes. In order to verify GateCycle, a simplified power plant system model was built under a certain ambient conditions in the design mode of Gatecycle and its performance was simulated under a series of different ambient conditions in the off-design mode. Meanwhile a Matlab code was written for calculating the performance of the same model built and simulated in GateCycle under the same ambient conditions, and the results were compared with each other.

In the design mode, the mass flow rate of the inlet ambient air that is required to condense the steam was calculated by both GateCycle and Matlab code for the given specifications of the Rankine cycle system and the equipment. And in the off-design mode, the condensing temperature in the air-cooled condenser was calculated and compared in both the GateCycle and Matlab codes.

### Problem Description

The power plant model was configured on a simplified Rankine cycle that consists of a steam turbine, an air cooled condenser, a pump and a boiler.

The Rankine cycle is designed according to the specifications listed in Table 1. The high and low pressures, as well as the mass flow rate of the steam will determine the Rankine cycle power generation. The inlet ambient air temperature and the inlet and outlet steam quality helps size the air-cooled condenser. The boiler efficiency affects the Rankine cycle efficiency. All the other parameters are set to be default values in GateCycle.

Table 1 Parameter set up for the equipment and the Rankine cycle

| Parameter Values | Description |
|---|---|
| $P_1$ =2300 kPa | Boiler pressure |
| $P_s$ = 10 kPa | Condensing pressure |
| $T_{a.in}$ = 0 °C | Inlet air temperature of ACC in the design mode |
| $X_{inlet}$ = 0.8 | Steam quality at the ACC inlet |
| $X_{outlet}$ = 0 | Steam quality at the ACC outlet |
| $M_s$ = 1 kg/s | Steam mass flow rate |
| $\eta_{boiler}$ =90% | Boiler efficiency |

In the design mode, the ambient condition is assumed to be 0 °C for the dry bulb temperature, and the mass flow rate of the ambient air is to be found based on these system specifications.

In the off-design mode, the ambient dry bulb temperature is arbitrarily selected to be 15 °C, and the condensing temperature is to be found for the specified air-cooled condenser. As mentioned above, the air-cooled condenser used the default surface provided by GateCycle, the details of which are shown in Table 2. The surface geometry will help determine the condensing temperature.

Table 2 The geometry configuration of the air cooled condenser

| ACC Parameters | Values |
|---|---|
| Face velocity of inlet air, $V_{air}$ | 3.8 m/s |
| Length of the ACC tubes | 7.0778m |
| Number of tubes per row, | 19 |
| Number of rows, | 3 |
| Outer diameter of the tubes | 25 mm |
| Inner diameter of the tubes | 21 mm |
| Diameter of the fin | 40 mm |
| Thickness of the fin, $s_{fin}$ | 1.016 mm |
| Pitch of the fin, $t_{fin}$ | 2.822 mm |
| $h_{fin}$, fin height | 20mm |

The GateCycle Model

The simple Rankine cycle was formed in GateCycle by connecting the icons of the boiler, steam turbine, air-cooled condenser and the pump, as shown in Figure 4. In the design mode, inputting the desired parameter values of the Rankine cycle and the equipment, the air mass flow rate for the air-cooled condenser and the heat transfer surface area of the air-cooled condenser was output. Then the Rankine cycle model was run in the off-design mode, where the cycle efficiency, condensing temperature and pressure in the air cooled condenser will be calculated under a different ambient dry bulb temperature of 15°C.

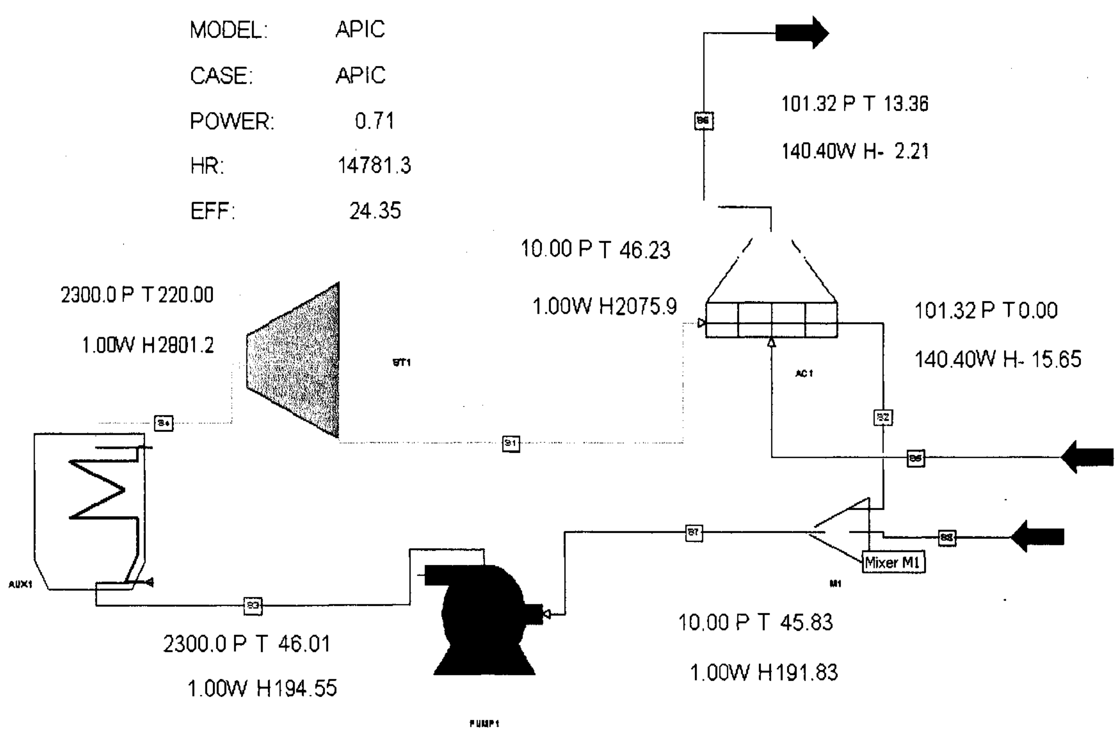


Figure 4 The Rankine cycle model scheme

## Matlab Code

Based on the parameters set up for the Rankine cycle and the equipment, calculations are carried out in both the design mode and off-design mode. In the design mode, the steam condensing temperature is assumed to be 45 °C, and the energy balance on the heat transfer process in the ACC gives

$$M_s h_{fg} X_{inlet} = M_a C_P (T_{a.out} - T_{a.in}) \tag{2.1}$$

where $C_p$ is the heat capacity of the air, kg/°C, and $M_a$ is the mass flow rate of the air, kg/s, and $X_{inlet}$ is the steam quality at the ACC inlet. Here the heat capacity of the air is $C_p = 1007 J/kg{\cdot}^\circ C$, and the specific enthalpy of evaporation is $h_{fg} = 2393 kJ/kg$. This is set by steam thermal properties at the saturation temperature of 45 °C. The air outlet temperature $T_{a.out}$ is assumed to be 15°C. Then the mass flow rate of the air could be obtained from this relationship.

The Nu number is given by

$$Nu_{air} = 0.134 C \,\mathrm{Re}_{air}^{0.681} \,\mathrm{Pr}_{air}^{1/3} \left( \frac{t_{fin} - s_{fin}}{h_{fin}} \right)^{0.2} \left( \frac{t_{fin} - s_{fin}}{s_{fin}} \right)^{0.1134} \tag{2.2}$$

where, C=0.36 for staggered tubes with 3 rows, $t_{fin}$ is the fin pitch, $s_{fin}$ is the fin thickness, and $h_{fin}$ is the fin height, which are all given by the surface geometry parameters (GateCycle help file), and Reynolds number is given by:

$$\mathrm{Re} = \frac{V_{air} D}{\gamma} \tag{2.3}$$

where $V_{air}$ is the air velocity m/s, D is the outer diameter of the tube, m , and $\gamma$ is the kinematic viscosity of the air, $m^2/s$.

Then the convection coefficient of the air side $h_a$ is given by:

$$h_a = \frac{Nu_{air} k}{D_o} \tag{2.4}$$

Since the h value of the steam side is much larger than that of the air side, the overall heat transfer coefficient U mainly depends on $h_a$, neglecting the thermal resistance of the tube wall, U could be reduced to

$$U = \frac{1}{\frac{1}{h_s} + \frac{1}{h_a} + RA} = h_a \tag{2.5}$$

Thus, with all the parameters known at this step, the heat exchange effectiveness $\xi$ could be obtained by the following relation:

$$\xi = q / q_{\max} = \frac{M_s h_{fg} X_{inlet}}{C_{\min}(T_{hot,in} - T_{cold,in}) M_a} \tag{2.6}$$

Then the $NTU$ (the Number of Transfer Units) is given by the relationship in equation 2.7 which is the simplified form for heat transfer with one fluid condensing.

$$NTU = \ln(1 - \xi) \tag{2.7}$$

Since the $NTU$ is defined by:

$$NTU = \frac{UA}{M_a C_p} \tag{2.8}$$

the required heat transfer surface area A could be determined using this relationship.

In the off-design calculation of the Matlab code, the ambient dry bulb temperature is assumed to be 15°C, which is the same as the GateCycle case. The $NTU$ method was also used to calculate the condensing temperature in the ACC based on the heat transfer surface area obtained above.

The $NTU$ could then be determined by equation 2.8 for the known heat transfer surface area A, and $\xi$ given by equation 2.7. Using an iterative method, the condensing temperature could be obtained from equation 2.6.

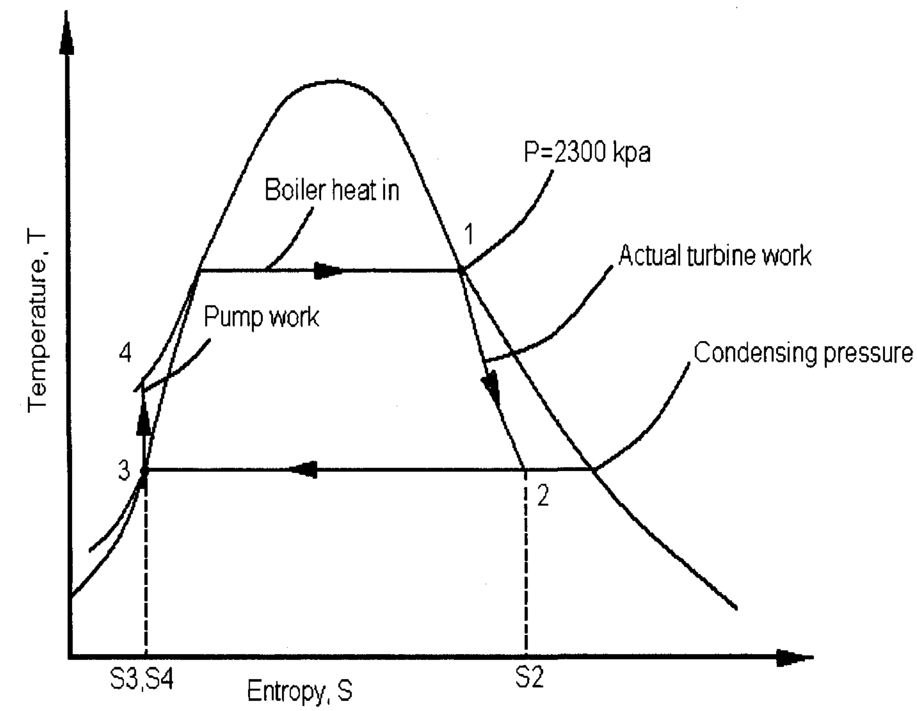


Figure 5 Rankine cycle T-s diagram

To calculate the cycle efficiency, an energy analysis was performed on the steam flow in the Rankine cycle. The T-s diagram of Rankine cycle is shown in the Figure 5, assuming that there is no pressure loss from state 4 to state 1 as well as from state 2 to state 3. Also the process 3 to 4 is assumed to be isentropic process.

The Rankine cycle efficiency is defined as the ratio of net work output and total heat coming into the system. From the Rankine cycle T-s diagram, it is clear that there are three parts of energy affecting that Rankine cycle efficiency, which are the turbine work output, the work consumed by the pump and the heat coming through the boiler. The net work output equals the turbine work output minus the pump work, and the total heat coming into the system is the heat absorbed in the boiler.

Since the steam quality and pressure are known at both the turbine inlet and outlet, the steam enthalpy could be obtained in the steam table, and the actual work done by the turbine was represented by:

$$W_{turbine} = M_s(h_1 - h_2) \tag{2.9}$$

where $h_1$ and $h_2$ could be found in the steam table, since the steam temperature and pressure are known at point 1, also the temperature and quality are known at point 2.

Thus the turbine work could be calculated by equation 2.9.

The work consumed by the pump is determined from the definition of the pump work.

$$W_P = v_m M_s(P_4 - P_3) \tag{2.10}$$

where the $P_3$ is the pressure at the pump inlet which equals to the condensing pressure $P_s$, $P_4$ the pressure at the pump outlet which equals to the boiler pressure $P_1$ and the mean specific volume $v_m$ is determined by taking average of the specific volume values at the inlet and outlet of the pump. Both of these can be obtained from the steam tables, once the steam pressure and quality are calculated at both inlet and outlet of the pump. Similarly, the steam enthalpy at the inlet and outlet of the boiler can also be found from the steam tables. Thus the heat provided to the boiler is determined by

$$Q_{in} = M_s(h_1 - h_4) / \eta_{boiler} \tag{2.11}$$

$\eta_{boiler}$ is the boiler efficiency which is 90%, and the Rankine cycle efficiency is calculated by

$$\eta = \frac{W_{net}}{Q_{in}} = \frac{W_{turbine} - W_P}{Q_{in}} \tag{2.12}$$

The Matlab code was written for the whole calculation, including the full state properties of the steam at 4 critical points shown in the Rankine cycle T-s diagram, which is attached in the Appendix.

## Results and Comparison

As previously described, the mass flow rate of the air was calculated under the design mode, as well as the condensing temperature and the Rankine cycle efficiency under the off-design mode. The results from GateCycle and Matlab codes are compared in the Table 3. The differences of the GateCycle results from the Matlab codes were calculated as well.

Table 3 Comparison of the results from GateCycle and Matlab Codes

| | GateCycle | Matlab Code | difference |
|---|---|---|---|
| $M_a$ (design mode) | 131.09 $kg/s$ | 127.63 $kg/s$ | 2.71% |
| $T_s$ (off-design mode) | 63 $^\circ C$ | 62 $^\circ C$ | 1.61% |
| $\eta$ (off-design mode) | 22.01% | 23.31% | 5.58% |

The results from GateCycle were not exactly the same but fairly close to those from the Matlab code and the differences are less than 6%. If further investigation of the difference between the results were desired, these differences might be due to some assumptions made in the Matlab code:

1. The pressure drop is neglected in the Matlab calculation, but the pressure drop of both sides was taken into consideration in Gatecycle.

2. There was sub-cooling occurring in the air cooled condenser and this decreased the Rankine cycle efficiency. In the Matlab codes, it is assumed that there is no sub-cooling in the air cooled condenser. So it is in the real operation, where sub-cooling is avoided as much as possible by adjusting the fan speed and the number of the working fans, but in GateCycle fans were assumed to run at a full speed and all the fans were working.

To further verify GateCycle results in the off-design mode, a comparison between GateCycle and Matlab code results are made on steam properties at 4 critical points as shown in the Rankine cycle T-s diagram. These steam properties are temperature, pressure and enthalpy of the steam.

Table 4 compares the steam properties at point 1. Point 1 is at the inlet of the steam turbine, where the temperature and pressure of the steam are preset to be the same in both the GateCycle and Matlab calculations. Since the enthalpy could be obtained directly from the steam tables for the given pressure and temperature, the small error between them may be due to the different database versions. This difference is only 0.04% and could be neglected.

Point 2 is at the turbine outlet and condenser inlet, where the steam quality was set to be 0.8. Thus the steam temperature has reached the saturated temperature under the given pressure at this point. Although the error of the temperature is 2.65% and the pressure is even higher, this didn't result in a high error in the enthalpy. The latter, among all the thermal properties, most directly influences the Rankine cycle efficiency, as shown in Table 5.

Table 4 Steam state properties comparison at the point 1

| | $T_1$ , °C | $P_1$ , kPa | $h_1$ , kJ/kg |
|---|---|---|---|
| Matlab code | 220 | 2300 | 2802.4 |
| GateCycle | 220 | 2300 | 2801.2 |
| Difference | N/A | N/A | 0.04% |

Point 3 is at the condenser outlet and pump inlet, which is right on the liquid saturation line on the Rankine cycle T-s diagram. Theoretically, the temperature at this point should be the same as that at point 2, as shown in Matlab code results in the Table 6. However, the temperature at this point in GateCycle shows a little decrease. This indicates that sub-cooling occurred in the air-cooled condenser, as noted earlier.

Although the enthalpy error of GateCycle at this point seems larger than that at point 2, the difference between Gatecycle and Matlab code value is 5.92 kJ/kg, which is actually much smaller compared to the difference of 21.6 kJ/kg at point 2.

Table 5 Steam state properties comparison at the point 2

| | $T_1$ , °C | $P_1$ , kPa | $h_1$ , kJ/kg |
|---|---|---|---|
| Matlab code | 62.32 | 22 | 2142.5 |
| GateCycle | 63.97 | 23.88 | 2164.1 |
| Difference | 2.65% | 8.55% | 1.01% |

Point 4 is at the pump outlet and also the boiler inlet, where the steam has the same pressure as at point 1. The difference of the temperature and the enthalpy are both within 3%, which is acceptable, as shown in Table 7.

Table 6 Steam state properties comparison at point 3

| | $T_3$ , °C | $P_3$ , kPa | $h_3$ , kJ/kg |
|---|---|---|---|
| Matlab code | 62.32 | 22 | 260.85 |
| GateCycle | 63.75 | 23.64 | 266.77 |
| Difference | 2.3% | 7.45% | 2.27% |

Table 7 Steam state properties comparison at point 4

| | $T_1$ , °C | $P_1$ , kPa | $h_1$, kJ/kg |
|---|---|---|---|
| Matlab code | 62.41 | 2300 | 263.15 |
| GateCycle | 63.95 | 2300 | 269.50 |
| Difference | 2.46% | 0 | 2.41% |

In summary, it appears that GateCycle is reliable to run a thermal cycle and give out results with acceptable differences to other types of calculations.

# CHAPTER 3

# DRY COOLING SYSTEMS MODELING

## Design Mode - Model Building

As it is mentioned in the Chapter 1, the major factor that affects the performance of dry cooling towers is the ambient dry bulb temperature. As the dry bulb temperature increases, the performance of a dry cooling tower decreases. This chapter is to find how the dry bulb temperature affects the performance of the dry cooling towers as well as the Rankine cycle efficiency.

A typical and simplified Rankine cycle with a conventional dry cooling system was established under the design mode in GateCycle.

The assumptions on which the Rankine cycle model was established are listed below:

1. All the equipment operates under steady state conditions [i.e., constant flow rates and fluid temperatures (at the inlet and within the equipment) which are independent of time].

2. The ambient conditions only affect the performance of the air-cooled condenser. Thus, when the ambient conditions changes, only the air-cooled condenser is running under the off-design mode, and performance of the other equipment is maintained under the design mode assumptions.

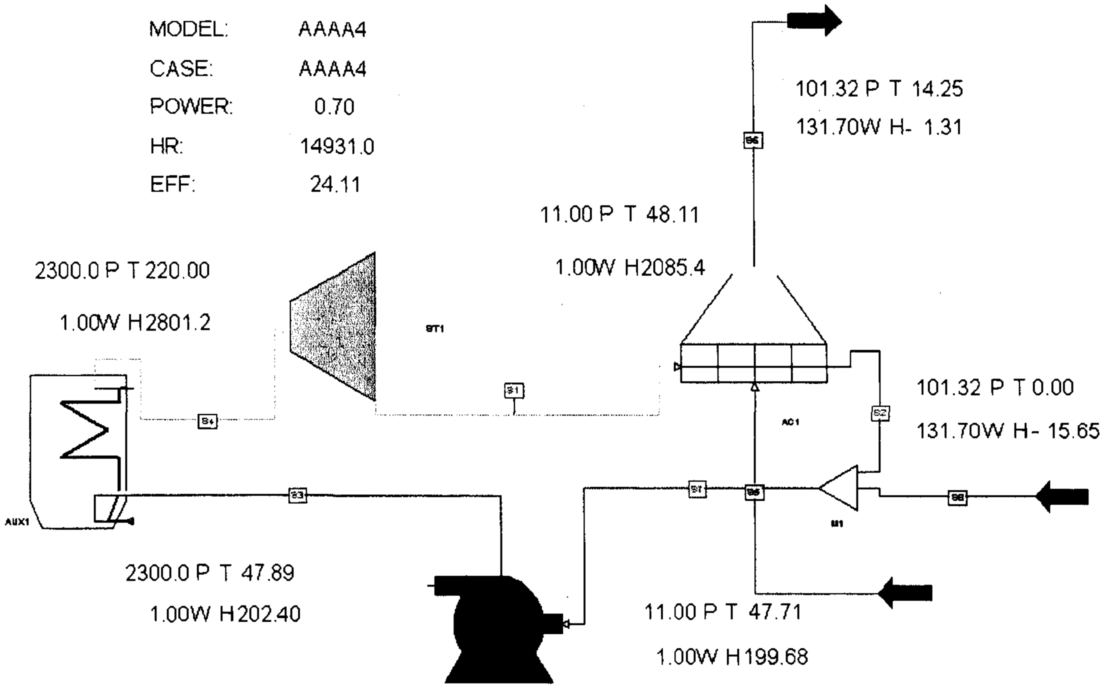


Figure 6 The model of Rankine cycle with the conventional dry cooling system

The computational modules for the turbine, pump, boiler and ACC (air cooled condenser) were picked from the module pools in GateCycle, and connected to form a Rankine cycle, shown in the Figure 6.

Under the design mode in GateCycle, equipment physical size (and other design parameters) and the Rankine cycle performance are calculated for the specified key parameters. The ambient dry bulb temperature under the design mode is 0 °C.

Similarly to the Rankine cycle model built in the previous case, the specified key parameters for the Rankine cycle are the high pressure and low pressure of the Rankine cycle as well as the steam mass flow rate. In addition, some specific requirements were also specified for the equipment. Table 8 shows all the preset parameters.

Table 8 The key specified parameters

| Key Specified Parameters | Values |
|---|---|
| Mass flow rate of the steam | 1 kg/s |
| Boiler pressure | 2300 kPa |
| Condensing pressure at the design mode | 11 kPa |
| Boiler efficiency | 90% |
| The steam quality at the turbine outlet | 0.8 |
| The steam quality at the boiler outlet | 1 |
| The steam quality at the air-cooled condenser outlet | 0 |
| Condensing temperature in the design mode | 48.11°C |

The condensing pressure was adjusted to make the Rankine cycle achieve the highest possible efficiency, the lower the condensing pressure is, the higher the Rankine cycle efficiency will be. 11 kPa is the lowest pressure that the air cooled condenser could reach under the conditions that all the equipment is working normally and the results could converge. And 48.11 °C is the resulting condensing temperature under the assumed condenser pressure of 11 kPa. A condensing pressure lower than 11 kPa would either result in the steam quality at the turbine outlet lower than 0.8 or an "exceeding the value of the stack temperature" warning at the air-cooled condenser outlet, as well as other accompanying side effects.

Design Mode – the Conventional Air-Cooled Condenser Design

During the design process of the conventional air-cooled condenser, all of the parameters are set to be the default values given by GateCycle.

The default surface for the air-cooled condenser is a circular-tube surface.

Some assumptions made for the air-cooled condenser design are listed below:

1. the fouling effects inside and outside the tubes are neglected;

2. The fin/tube bond resistances are neglected;

3. All the condensing bays operate in co-current mode, in which the incoming steam flows in the same direction as the condensate along the tube walls, and all of the steam is assumed to be condensed in these co-current bays. So this is a simple air-cooled condenser with the basic configuration.

4. The steam is condensed completely at the outlet of the air-cooled condenser with the same pressure as the inlet.

Figure 7 shows the main setting window of the conventional air-cooled condenser. This computational module could serve as either air cooler or air - cooled condenser, and the latter is what we need.

The air- and water-sides use separate design methods. On the water side, the desired saturation pressure value is required to be specified; and on the air side, one of the four parameters is to be specified among heat exchange surface, mass face velocity(mass flow rate, kg/s), face velocity(velocity, m/s) and tube length, and the rest will be calculated accordingly. The suggested procedure for determining these for an unknown air-cooled condenser is to initially specify one of the velocity parameters empirically. Then select the number of bays such that the resulting tube length is somewhere between 3 and 12 m (12 and 40 ft). At this stage, enter reasonable numbers for the tube length and the number of tubes per row. Then the heat exchange surface area could be determined at the final stage.

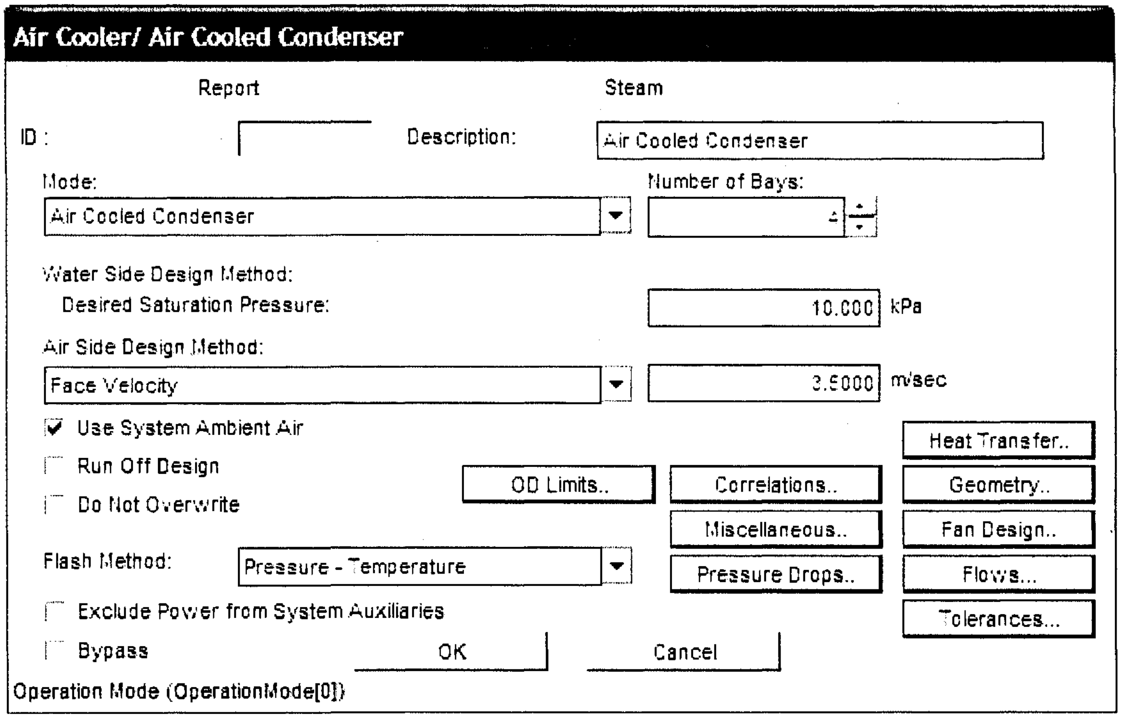

Figure 7 The main set up window of the conventional air-cooled condenser

Meanwhile, several categories of parameters could also be specified for the ACC, such as the parameters of heat transfer, geometry, fan design, pressure drops and the tolerances, which are in the sub settings windows, shown as a button link in the main setting window.

Parameter settings for heat transfer, geometry, miscellaneous and pressure drops are shown in the Appendix.

## Off-Design Mode Simulation - Results and Discussion

The performances of the Rankine cycle as well as the conventional ACC were simulated under the off-design mode.

In the off-design mode, the ambient dry bulb temperature is varied from 5 °C to 40 °C. The influence of the ambient dry bulb temperature on the condensing temperature is plotted in Figure 8. A linear increase of the condensing temperature is shown as the ambient dry bulb temperature increases. The condensing temperature reaches as high as 90 °C, when the ambient dry bulb temperature goes up to 40 °C. And it shows a continuously increasing trend when the ambient temperature is even higher than 40 °C. In a location like Las Vegas, where summer temperature often stays above 40 °C for long periods, the air-cooled condenser would have to keep working under a condensing temperature higher than 90 °C.

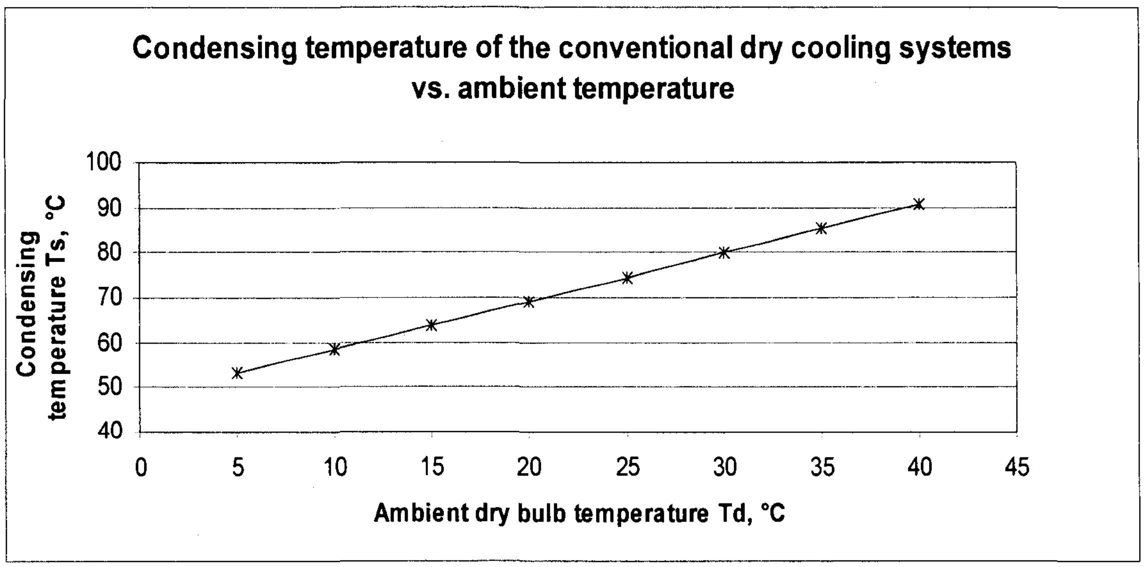


Figure 8 The condensing temperature of the conventional dry cooling system vs. the ambient temperature

The condensing pressure variation with the ambient dry bulb temperature can be deduced from the Figure 8, since the pressure is a function of the temperature only when the steam is at the saturation state. Figure 9 shows a nonlinear continuously increasing of the condensing pressure as the ambient dry bulb temperature increases.

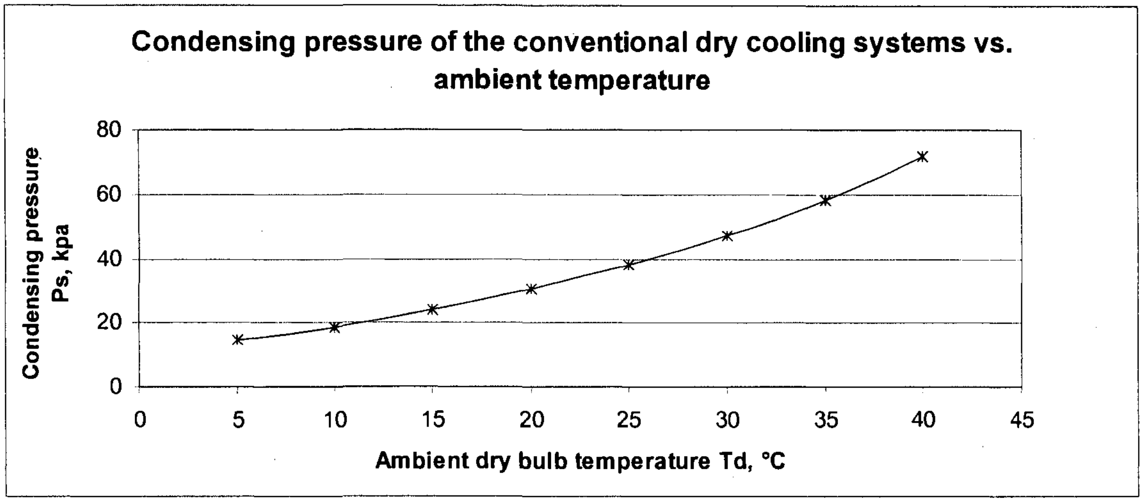


Figure 9 The condensing pressure of the conventional dry cooling system vs. ambient temperature

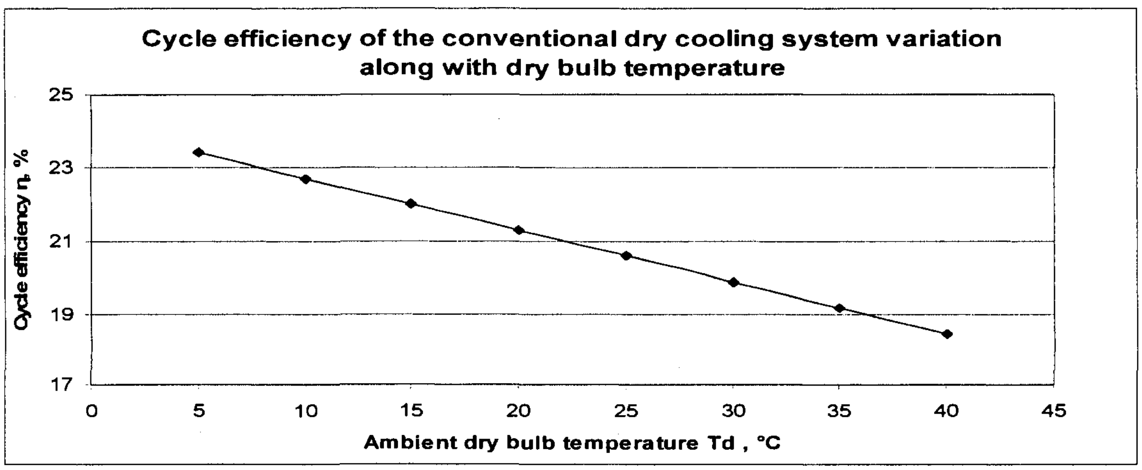


Figure 10 The cycle efficiency vs. ambient temperature for a power plant with a conventional dry cooling system

Since the turbine outlet pressure is limited by the condensing pressure, the increase of the condensing pressure leads to a decreasing turbine output and, in turn, the Rankine cycle efficiency. Figure 10 indicates a great decrease in Rankine cycle efficiency as the ambient dry bulb temperature rises. As shown here, during the winter time when the ambient temperature goes down to 5 °C, the efficiency of the power plant is around 23.4%. During the summer when the ambient temperature could reach as high as 40 °C in Las Vegas, the efficiency of the power plant could decrease 21.4% compared to that of 18.44% in the winter.

## Conclusion

In short, the ambient dry bulb temperature is a very important factor that affects the performance of the Rankine cycle. As it increases, the condensing temperature and pressure continuously increase and the Rankine cycle efficiency decreases accordingly. Fortunately, what the figures show are the results for a simple Rankine cycle. For a more complicated power plant system with appropriate component additions, the efficiency would be different and the sensitiveness to the ambient temperature might decrease, as is noted earlier in this paper.

CHAPTER 4

# COMPARISON WITH WET COOLING MODEL

## Design Mode - Model Building

Different from dry cooling systems, the ambient condition that affects the performance of wet cooling systems is the ambient wet bulb temperature, i.e. both the dry bulb temperature and the relative humidity. Figure 11 shows the difference of the dry and the wet bulb temperature under different relative humidity.

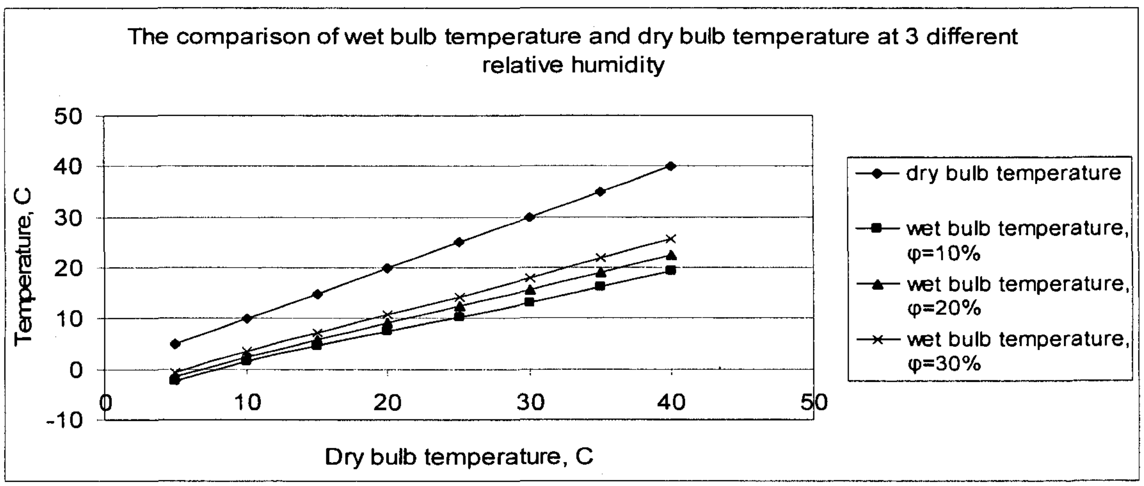


Figure 11 The comparison of dry bulb temperature and wet bulb temperature with various relative humidities

It is obviously that the dry bulb temperature is always higher than the wet bulb temperatures, the lower the relative humidity is the bigger the difference is between the dry and wet bulb temperatures. Moreover, as the dry bulb temperature increases, the difference between them also increases. These observations explain well why the Rankine cycle with wet cooling systems is usually more efficient than that with the dry cooling systems, especially during the summer time.

In this chapter, the Rankine cycle with the conventional wet cooling counterpart was simulated in GateCycle, as a comparison with the conventional dry cooling system model. In addition, ideal cases were also built for each cooling systems, and the Rankine cycle efficiency variation under the different ambient conditions was studied of these cases. And a yearly power generation for each case was further calculated using the TMY2 hourly data.

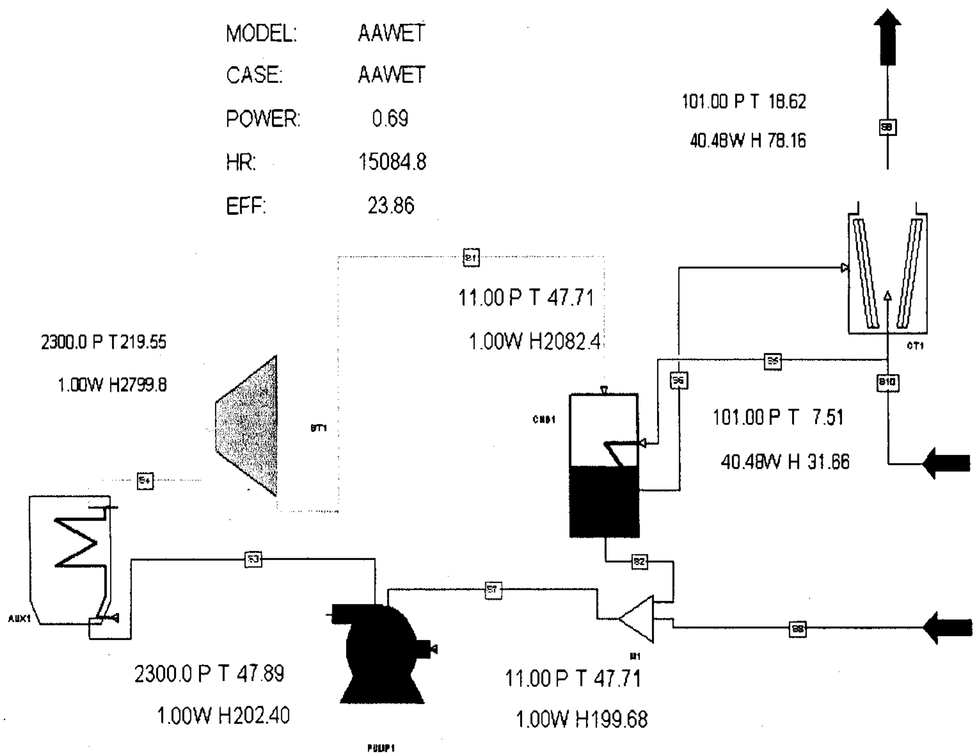


Figure 12 The model of Rankine cycle with the conventional wet cooling system

Figure 12 shows the Rankine cycle model with the conventional wet cooling system built in GateCycle, including the pump, boiler, steam turbine, conventional wet cooling tower and the condenser.

On what basis will the comparison between dry and wet cooling systems be? Backer and Wurtz (2003) showed in their paper the performances of three typical cooling systems designed for the same power plant: 100% wet cooling system, 100% dry cooling system and the parallel condensing system (PCS), which is the combination of former two systems. The steam turbine back pressure was plotted with respect to the ambient dry bulb temperature for the three cooling systems, as shown in the Figure 13.

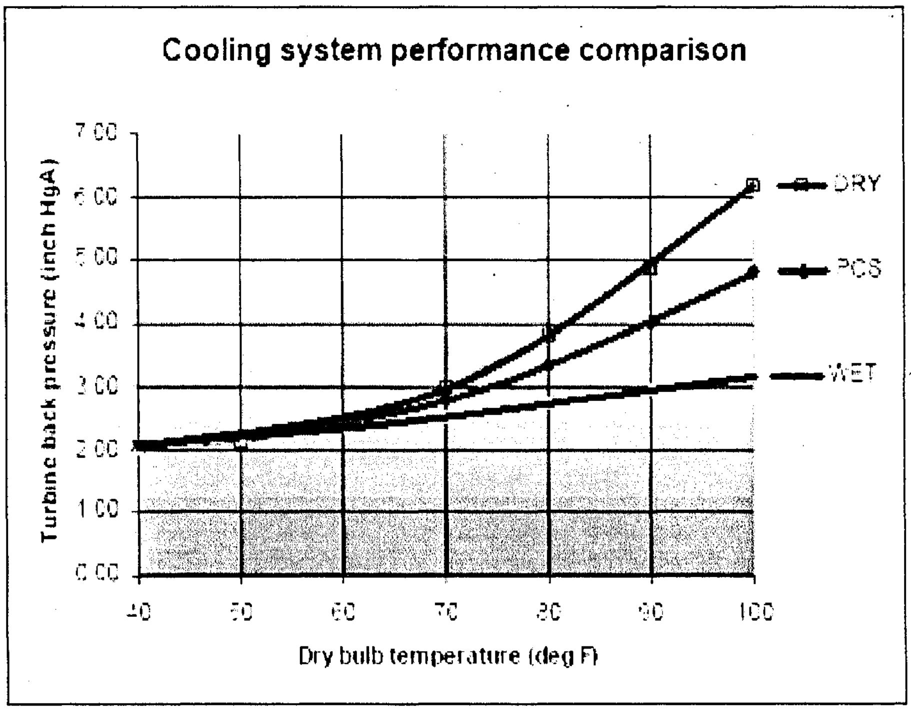


Figure 13 Dry, PCS and wet cooling systems – comparison of the performance. (Backer and Wurtz, 2003]

The PCS is not included in the discussions in this paper, but the performance of other two systems indicates a fact that under a low ambient temperature of around 60 degree F, the wet and dry systems result in almost the same turbine back pressure. Based on this point, the ambient conditions in the wet cooling design will be chosen as 0 °C for the ambient dry bulb temperature and 10% for the relative humidity, and the condensing pressure will be as close as possible to that of the dry cooling model under the same design conditions.

In addition, the Rankine cycle with the wet cooling counterpart was also built under the same assumptions (see Chapter 3) and other parameters settings were the same as seen in Table 8.

### Design Mode – the Conventional Wet Cooling System Design

Similarly to the dry cooling model, all the parameters in the conventional wet cooling model were set to be default values given by GateCycle in the design process.

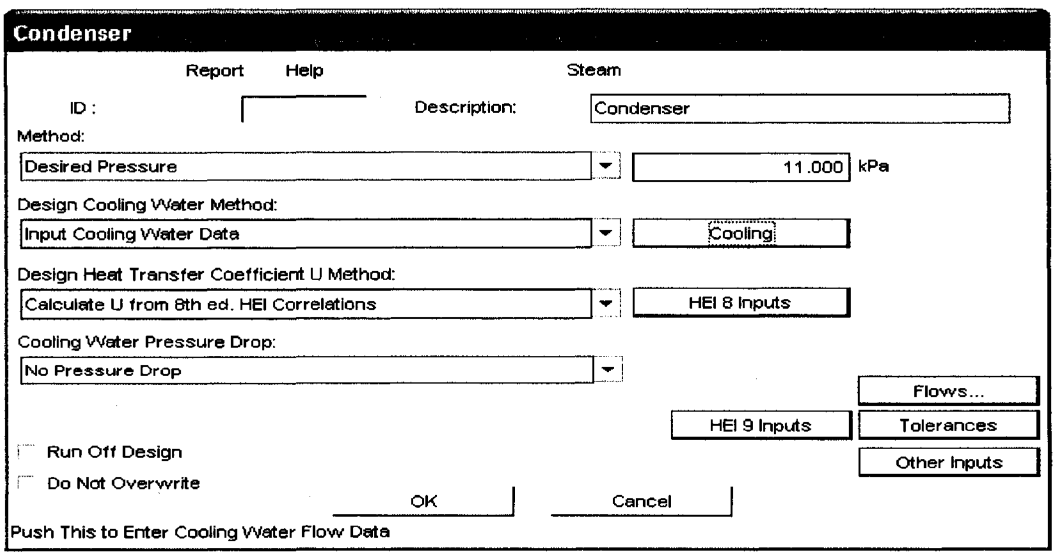

Figure 14 The main setting window of the condenser

The assumptions that were made in the conventional wet cooling system design are listed below:

1. The outlet of the condenser is saturated liquid at the same pressure as the inlet flows.

2. The condenser and the wet cooling tower are working under the steady state with steady flow.

Figure 14 and Figure 15 show the main configuration setting windows of the wet cooling part, including the condenser and the wet cooling tower.

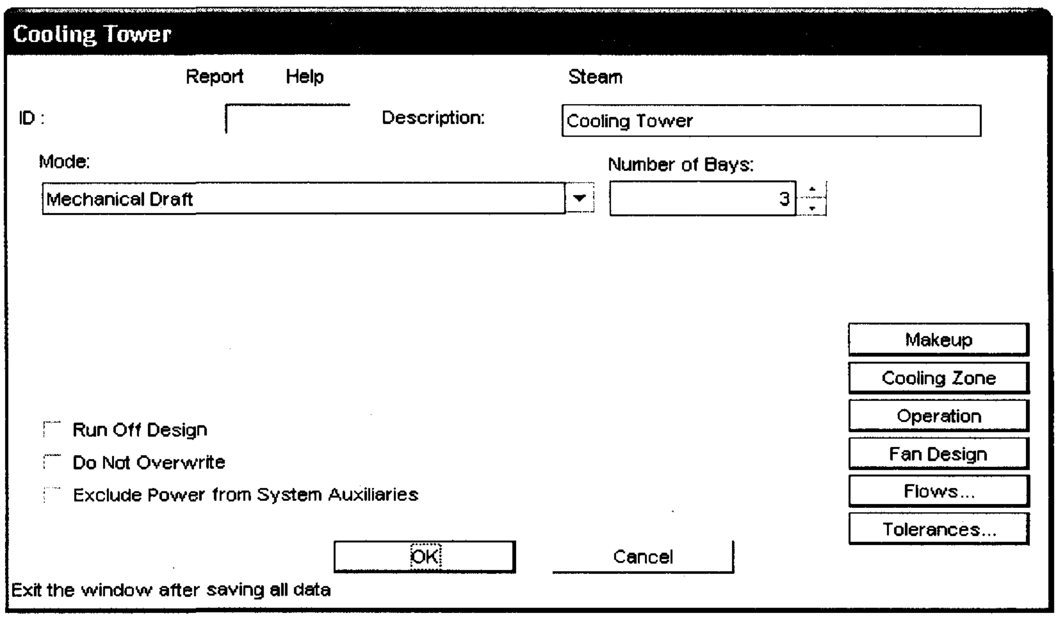


Figure 15 The main setting window of the cooling tower

As is mentioned in the last section, the desired pressure in the condenser was set to be 11 kPa. To achieve this, the air to water ratio in the cooling zone of the wet cooling tower was adjusted to 1.2. Other parameters were all set to be default values.

The parameter settings for the cooling zone, heat transfer and pressure are seen in the Appendix.

## Off Design Mode - Results and Discussion

In the off design mode, the conventional wet cooling model was run under different ambient conditions, where the ambient dry bulb temperatures were varied from 5 °C to 40 °C under relative humidities of 10%, 20% and 30%, respectively. The performance of the Rankine cycle was determined and plotted.

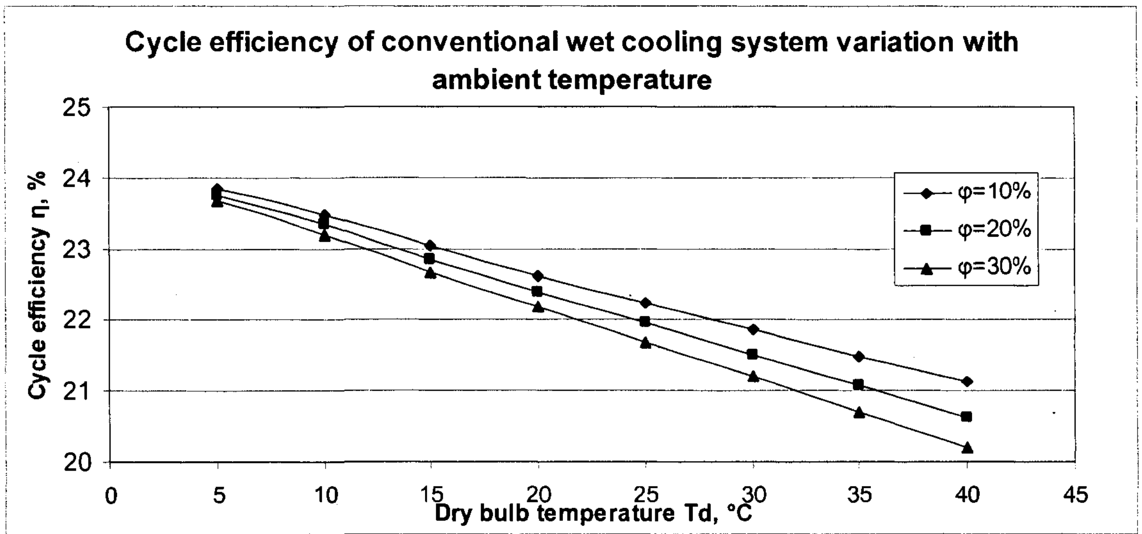


Figure 16 Cycle efficiency of the conventional wet cooling system variation with ambient temperature and relative humidity

As the ambient dry bulb temperature increases, Figure 16 shows a similar decreasing trend of the Rankine cycle efficiencies for the conventional wet cooling model under all different relative humidities. It also shows that at the same ambient dry bulb temperature, the Rankine cycle efficiency decreases as the relative humidity increases. But even under the highest relative humidity considered here, the Rankine cycle with the conventional wet cooling system is still more efficient than that with the conventional dry cooling system. Consider the point at the ambient dry bulb temperature of 40 °C. Here the cycle efficiency of the dry cooling system case is 18.44%, but for the wet cooling counterpart under a relative humidity of 30%, the cycle efficiency is 20.2%. Moreover, it is observed that relative humidity has a greater impact on Rankine cycle efficiency at higher ambient temperatures.

## Comparison of Ideal Cases and Conventional Cases

From the calculations of the heat transfer process of the dry cooling system in Chapter 2, the overall heat transfer coefficient U is found to be very low, due to the high thermal resistance on the air side, which greatly limits the heat transfer efficiency of the dry cooling system. If the thermal resistance between the steam and the air could be zero, that is no energy loss in the heat transfer process, the cooling systems would ideally reach the possible maximum heat transfer efficiency.

In this section, such an ideal case is studied for each cooling system in order to see how much different it is from the conventional case performance. The ideal dry cooling system is defined as that where the condensing temperature is equal to the ambient dry bulb temperature. Similarly, the ideal wet bulb temperature is defined as that where the condensing temperature equals to the wet bulb temperature for the wet cooling counterpart. In each dry cooling system case, performance of the Rankine cycle under different dry bulb temperatures was studied, and in each wet cooling system case, the impact of both dry bulb temperature and relative humidity was included.

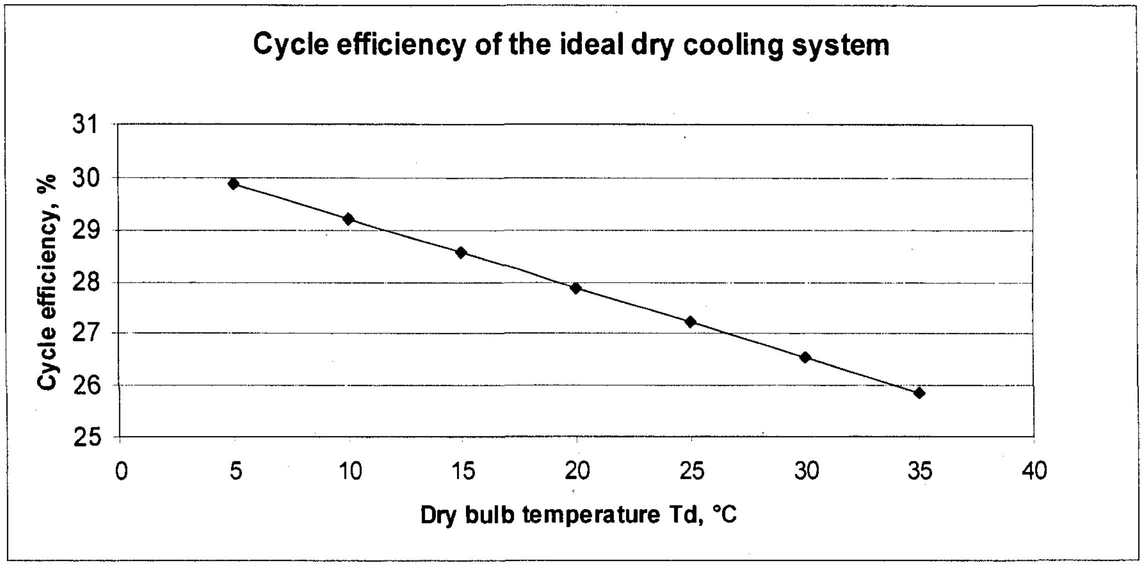


Figure 17 Cycle efficiency of the ideal dry cooling system variation with ambient temperature

Figure 17 shows a similarly decreasing trend of the cycle efficiency under increasing ambient dry bulb temperature for the ideal dry cooling system. However, the Rankine cycle efficiency of the power plant with the ideal dry cooling system is much higher than that with the conventional dry cooling system. Even under the dry bulb temperature of 40 °C, the cycle efficiency of the Rankine cycle with the ideal dry cooling system can still be 25.2%, which increases about 37% compared to 18.44% for the conventional dry system under the same ambient temperature. Note that this yields the same results in Figure 18 for the ideal wet cooling counterparts. It is found that the power plant with an ideal dry cooling system could reach a comparable efficiency to that of the ideal wet cooling system. This gives us hope that a dry cooling system could perform nearly as well as the wet cooling system, even in the severely hot days.

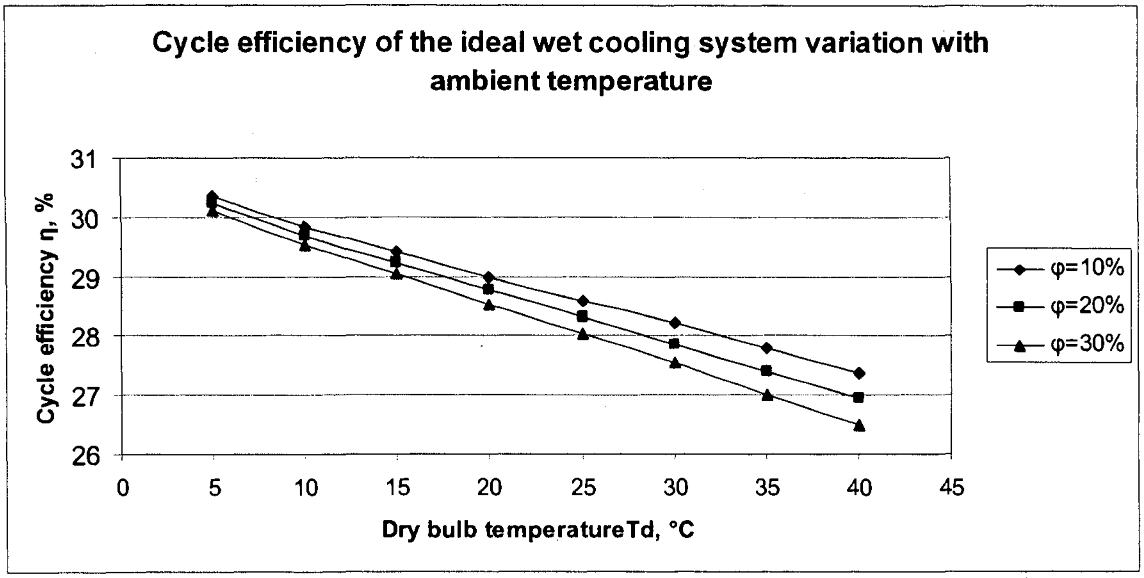


Figure 18 Cycle efficiency of the ideal wet cooling system variation with ambient temperature and relative humidity

## Hourly Performance Calculation Using TMY2 Data

TMY2 are data sets of hourly values of solar radiation and meteorological elements for a 1-year period, among which the DNI, dry bulb temperature and relative humidity hourly data were used for calculating the hourly performance and total power generation for four cases: Rankine cycles with the conventional dry cooling system, the ideal dry cooling system, the conventional wet cooling system and the ideal wet cooling system.

The energy generated by the Rankine cycle in an hour is calculated using the following relationship with the hourly data:

$$P=DNI*\eta_r*\eta_{boiler}*\eta*3600/1000 \tag{4.1}$$

where DNI is the direct normal incidence hourly data, W/m$^2$, $\eta_r$ is the collector efficiency, which is 0.73; $\eta_{boiler}$ is the boiler efficiency, which is set to be 0.9 in GateCycle; $\eta$ is the Rankine cycle efficiency, and 3600/1000 is to convert the units to kWh.

In order to calculate hourly Rankine cycle efficiency using TMY2 data for each case, relationships between Rankine cycle efficiency $\eta$ and the ambient conditions were developed for dry cooling systems and wet cooling counterparts separately.

In the conventional and ideal dry cooling system cases, the ambient dry bulb temperature is the only variable that affects the Rankine cycle performance. With this in mind, the relationship between the Rankine cycle efficiency and ambient temperature could be easily obtained from Figure 10 and Figure 17:

For the conventional dry cooling system case:

$$\eta_{d,c} = -0.1468\, T_d + 22.526 \tag{4.2}$$

and for the ideal dry cooling system case:

$$\eta_{d,i} = -0.1324\, T_d + 30.503 \tag{4.3}$$

In wet cooling systems, both dry bulb temperature and relative humidity are considered at the same time. The Rankine cycle efficiency is assumed to be a linear function of dry bulb temperature, where the coefficients are assumed to be a function of relative humidity.

$$\eta_{w,c} = a_c(\varphi)\, T_d + b_c(\varphi) \tag{4.4}$$

$$\eta_{w,i} = a_i(\varphi)\, T_d + b_i(\varphi) \tag{4.5}$$

Then for the conventional wet cooling system, the Rankine cycle efficiency as a function of both dry bulb temperature and relative humidity is obtained from Figure 6:

$$a_c(\varphi) = -0.102\,\varphi - 0.0684 \qquad (4.6)$$

$$b_c(\varphi) = -0.305\,\varphi + 24.26 \qquad (4.7)$$

Similarly for the ideal wet cooling system:

$$a_i(\varphi) = -0.095\,\varphi - 0.074 \qquad (4.8)$$

$$b_i(\varphi) = -0.480\,\varphi + 30.75 \qquad (4.9)$$

With the relationships above, the hourly Rankine cycle efficiency for each case could be obtained from the TMY2 data for Las Vegas. And the total energy generated in a whole year is the sum of the hourly energy generation, as shown in the Table 9.

Table 9 Comparison of yearly energy generation of power plants with different condenser systems based on TMY2 weather data

| Power Plant Cases | Energy Generation in a Whole Year Per Unit Area of the Receiver (MWh) |
|---|---|
| With conventional dry cooling system | 38.2 |
| With conventional wet cooling system | 43.4 |
| With ideal dry cooling system | 54.2 |
| With ideal wet cooling system | 55.8 |

It is obvious that the power plant with ideal cooling systems generate more energy than those with the conventional ones in a whole year, and those with the dry cooling systems generate less energy than their wet counterparts. However, the yearly energy generated by the ideal dry cooling case is very close to the ideal wet cooling case, which indicates the potential of the power plant with the conventional dry cooling system performing nearly as well as that with the wet cooling system.

## Conclusion

Generally speaking, the Rankine cycle with the dry cooling system is less efficient than that with the wet cooling system, especially when the ambient temperature is high. There are two major reasons result in this, first, the thermal resistance of the air side is much larger than the steam side, which limits the overall heat transfer coefficient; secondly, the dry bulb temperature is always higher than the wet bulb temperature, which results a higher condensing pressure in the air cooled condenser, thus lowering the Rankine cycle efficiency. In the ideal case simulations, where the first reason was eliminated arbitrarily, the performances of the Rankine cycles with the ideal dry cooling system and ideal wet cooling system are much closer and higher than their conventional counterparts. This also gives us hope that an enhanced dry cooling system could perform nearly as well as the conventional wet cooling system.

# CHAPTER 5

## AN ADVANCED CIRCULAR-TUBE SURFACE STUDY

### New Surface Introduction

As mentioned in the previous chapters, all the cases were run based on the default surface configuration for the condenser heat exchange equipment. In this section, an advanced real surface was selected and applied to the conventional dry cooling system, and the Rankine cycle with the new air cooled condenser was simulated in the GateCycle as the previous cases did.

A comprehensive comparison method of compact heat exchanger surface is described in Kahlil's thesis (Khalil, 2006). It is well known that a compact heat exchange surface, a high heat transfer rate, a small weight, a low pumping power and capital cost are the desired characteristics of a good surface. In this study, the heat transfer rate and the compactness will be the major factors considered on the new surface selection.

Direct test data of the geometry and physical parameters for some compact heat exchanger surfaces are provided by Kays and London (1998). The friction factor and the heat transfer characteristic $St*\Pr^{2/3}$ are plotted versus Reynolds number, with the geometrical parameters specified for each surface as well. Among 16 different circular-tube surfaces with circular fins provided in the book, the one with the highest $St*\Pr^{2/3}$ value was applied to the dry cooling system.

The geometry parameters of the new surface and default surface are compared in the Table 10. Since the inner diameter of the tube isn't provided in the book, a default gauge value of 1.27mm given by GateCycle is used to calculate it.

Table 10 Geometries of two different surfaces

| Geometry parameters | Default surface | New surface |
|---|---|---|
| Tube outer diameter (mm) | 25.4 | 26.01 |
| Hydraulic outer diameter (mm) | 25.4 | 26.01 |
| Gauge (mm) | 1.27 | 1.27 |
| Pitch/outer diameter (normal to flow) | 2.5 | 2.0146 |
| Pitch/outer diameter (in the flow) | 2.1667 | 3.001 |
| Fin diameter (mm) | 40 | 44.2 |
| Fin thickness (mm) | 1.0160 | 0.305 |
| Fin pitch (mm) | 2.8220 | 2.89 |

The pitch/outer diameter in this table is defined to be the ratio of the pitch and the outer diameter of the tube, and there are two types of values when looking from the different directions, one is normal to the flow and the other is in the direction of the flow, as shown in the Figure 19.

With this new surface applying to the conventional air-cooled condenser, the previous Rankine cycle was rebuilt in GateCycle under the same ambient conditions, as well as the same geometry parameter settings of all the other equipment. This new Rankine cycle model was run in two cases. In the first case, the heat transfer surface area was kept the same as the default conventional dry cooling system; in the other case, the heat transfer surface area was doubled in the new conventional dry cooling system.

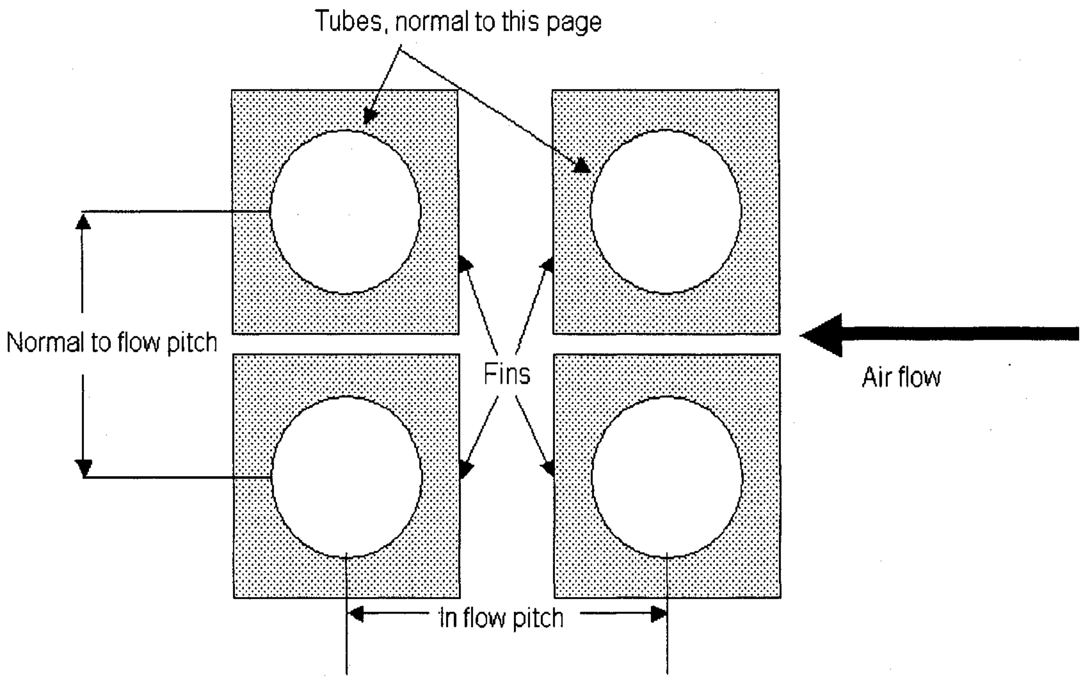


Figure 19 Pitch/outer diameter which is normal to the flow or in the flow

Case 1 – Equal Surface Area

In the conventional wet case, the wet cooling part was sized to achieve the same condensing pressure as the conventional dry case for comparison. On the contrary, the AAC in case 1 was designed to have the same heat transfer surface area as the default one, and the according condensing pressure was then calculated under the design mode. The parametric design of the Rankine cycle model with the new air-cooled condenser is shown in the Table 11. Most parameters were set the same as the default model, except that the condensing temperature was lowered to 41.92 °C, compared to 48.11°C for the default conventional dry cooling case, and the condensing pressure was accordingly brought down to 8.16 kPa, compared to 11 kPa for the default case.

Table 11 The parameters set up of the new Rankine cycle for case 1

| Rankine Cycle Parameters | Value |
|---|---|
| Mass flow rate of steam | 1 kg/s |
| Boiler pressure | 2300 kPa |
| Condensing pressure at the design mode | 8.16 kPa |
| Boiler efficiency | 90% |
| The steam quality at the turbine outlet | 0.8 |
| The steam quality at the boiler outlet | 0 |
| The steam quality at the air-cooled condenser outlet | 1 |
| Condensing temperature at the design mode | 41.92 °C |

A number of tests were run for this case under different ambient dry bulb temperatures in the off-design mode. The results were plotted versus ambient dry bulb temperature and compared with those of the default case, shown in Figure 20, Figure 21 and Figure 22.

Figure 20 compares the condensing temperature in the new ACC with that in the default one. The condensing temperature in the new ACC shows a small but definite decrease under all the temperatures. The condensing temperature of the new ACC lowered to 83.94 °C, which decreases 7.4% compared to 90.65 for the default case, when the ambient dry bulb temperature reaches 40 °C. And the condensing temperature decreases an average of 9.7% over all the ambient dry bulb temperatures.

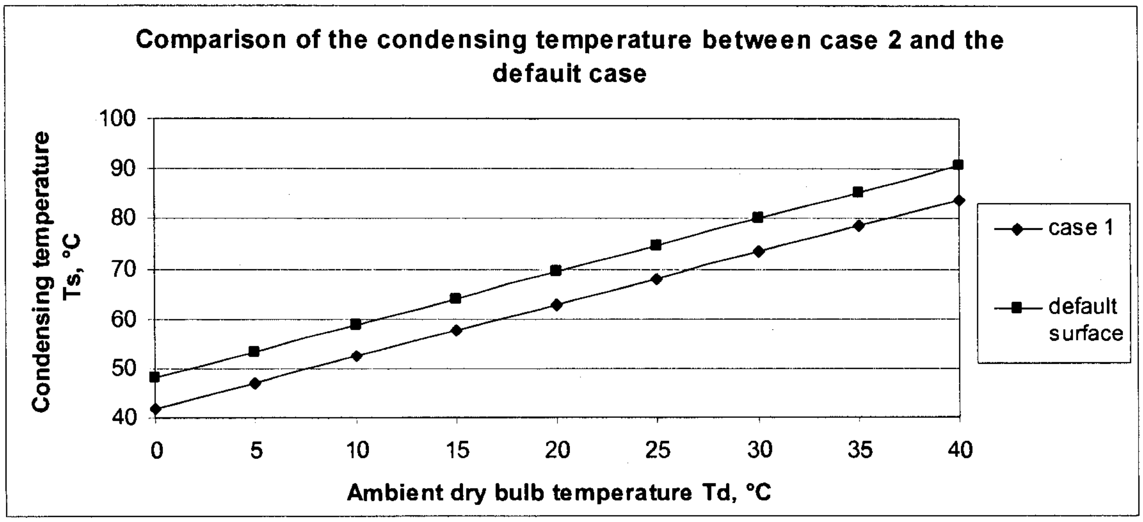


Figure 20 Condensing temperature comparisons between case 1 & default case

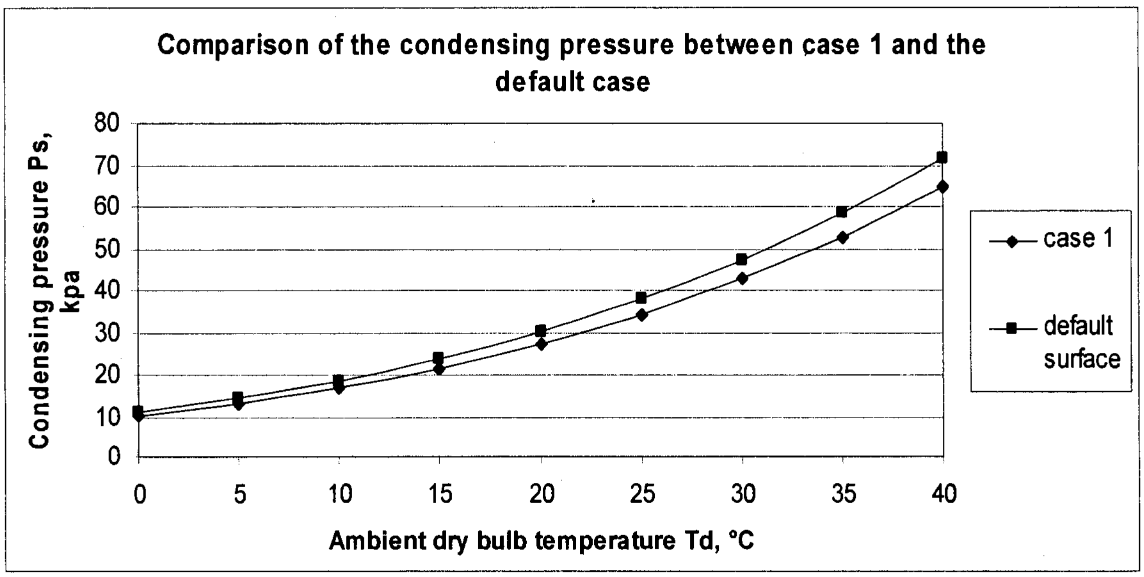


Figure 21 Condensing pressure comparisons between case 1 & default case

Figure 21 compares the condensing pressure variation between the new ACC and default one versus the ambient dry bulb temperature. A condensing pressure decrease in the new ACC is indicated. Although the difference looks small between the two curves, the condensing pressure of the new ACC decreases 25% on average compared to the default case over all the ambient temperatures.

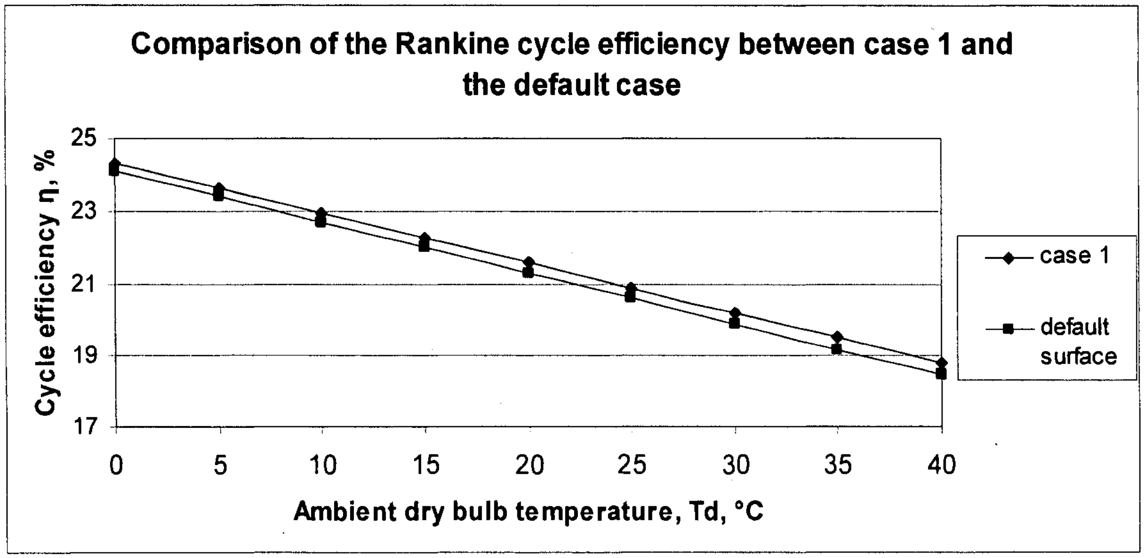


Figure 22 Comparison of the cycle efficiency between case 1 and the default case

Figure 22 compares the Rankine cycle efficiency of two power plants with the new ACC and the default one. The cycle efficiency of the power plant with the new ACC increases 3.9% on average compared to that with the default ACC.

Case 2 – Double Surface Area

In this case, the heat transfer surface area was doubled. As a result, the lowest condensing pressure that the air-cooled condenser could reach in the design mode was 4.08 kPa, and the according condenser temperature was brought down to 29.33 °C. All the other parameters were set to be the same as case 1, which are shown in the Table 12.

Table 12 The parameters set up for the Rankine cycle in case 2

| Rankine cycle Parameters | Value |
|---|---|
| Mass flow rate of steam | 1 kg/s |
| Boiler pressure | 2300 kPa |
| Condensing pressure at the design mode | 4.08 kPa |
| Boiler efficiency | 90% |
| Turbine efficiency | 90% |
| Quality of the steam at the outlet of the boiler | 0 |
| Quality of the steam at the outlet of the air-cooled condenser | 1 |
| Condensing temperature at the design mode | 29.33 °C |

Similar tests of the Rankine cycle with the new dry cooling system with doubled heat transfer surface area are run under various ambient dry bulb temperatures. Comparisons of the results are made between the case 2 and the default case in Figure 23, Figure 24, and Figure 25.

Figure 23 compares the condensing temperature between case 2 and the default case. Both cases show a similar increasing trend of the condensing temperature as the ambient temperature increases, but case 2 shows an apparently lower condensing temperature. The condensing temperature of case 2 reached 70.94 °C, which decreased 21.7% compared to 90.65 °C for the default case, when the ambient temperature reaches 40 °C. And the condensing temperature of case 2 decreases about 28.8% on average compared to the default case.

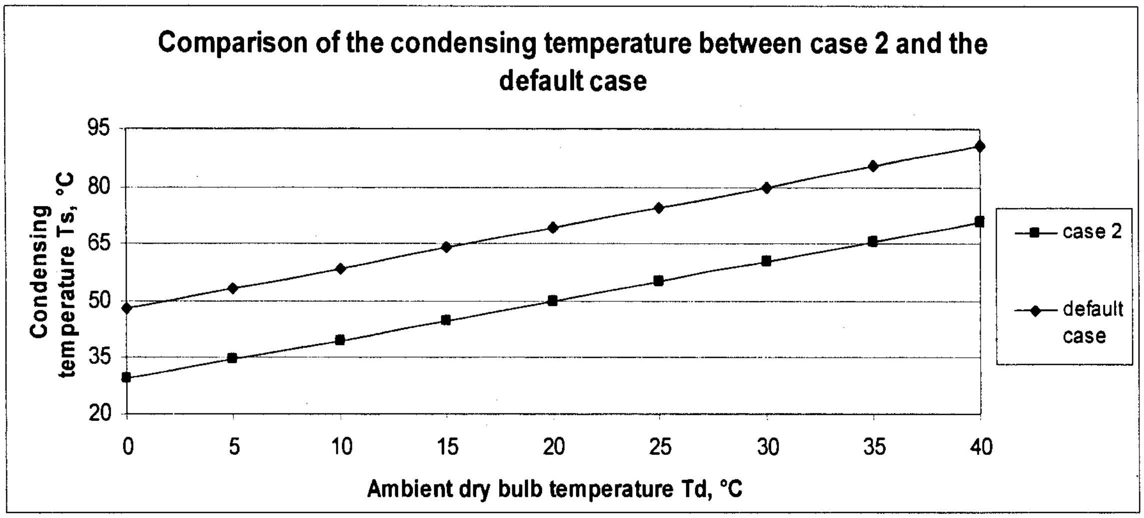


Figure 23 Comparison of the condensing temperature between case 2 and the default case

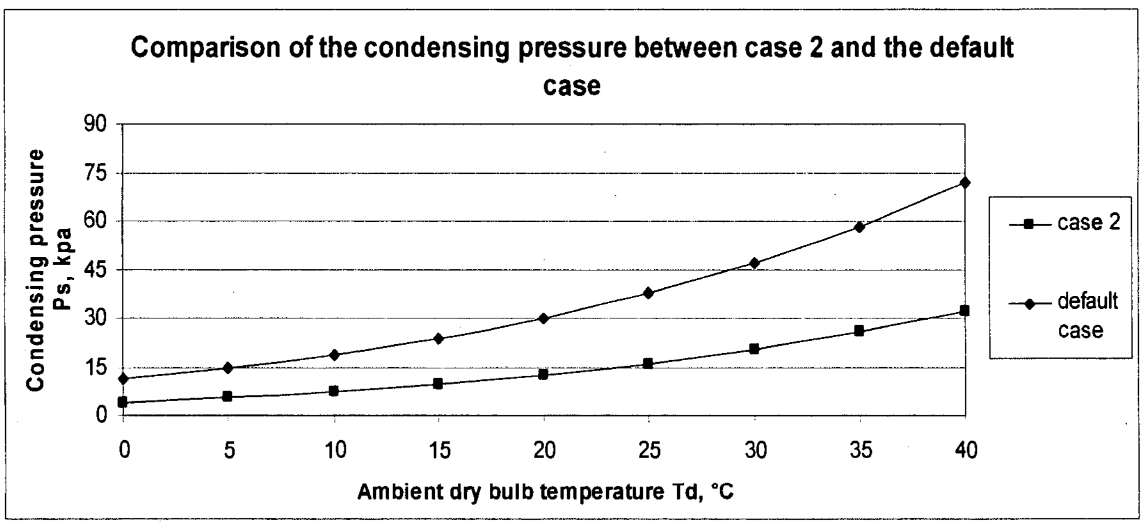


Figure 24 Comparison of the condensing pressure between case 2 and the default case

Figure 24 shows an increasing trend of the condensing pressure in both cases. However, it can be seen that the condensing pressure in the case 2 increases much more slowly than the default case. It also shows an obviously lower condensing pressure of case 2 compared to the default case under all ambient temperatures. The condensing pressure in case 2 reaches 32.45 kPa, which lowers about 54.8% compared to 71.86 kPa in the default case, when the temperature reaches 40 °C. And it lowers 59.1% on average comparing to the default case.

Figure 25 compares the Rankine cycle efficiency of case 2 and the default case. And it shows an average of 11.9% increase in the Rankine cycle efficiency in case 2 compared to the default case.

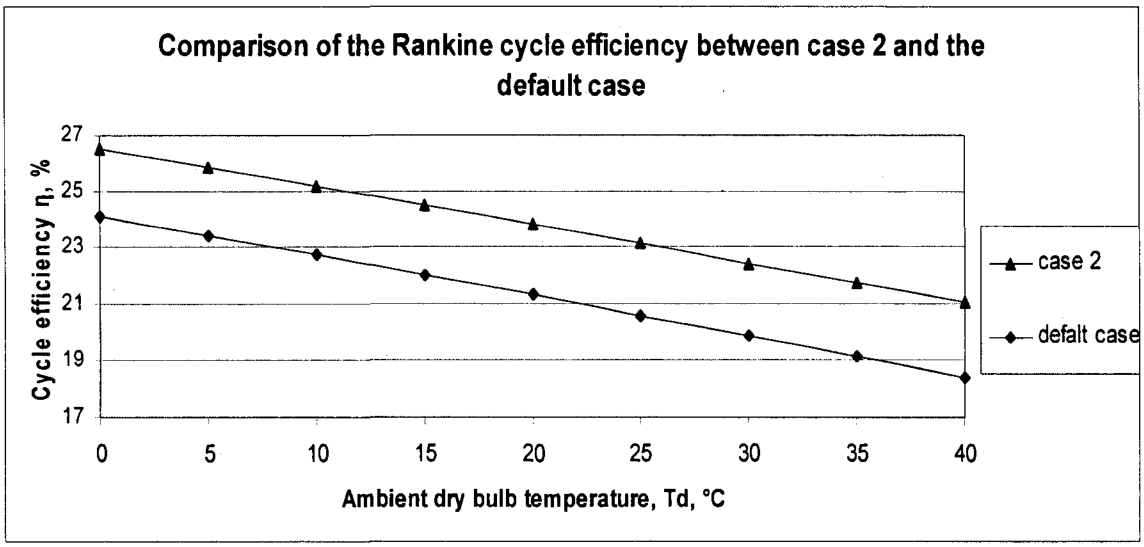


Figure 25 Comparison of the cycle efficiency between case 2 and the default case

Comparison of Case 1 and Case 2

To make it more pronounced, ratios of the new-surface case results (case 1 and case 2) and the default-surface case results are displayed in Table 13,Table 14 and Table 15.

Table 13 shows the ratio of the condensing temperature in case 1 and case 2 with respect to the default case. The ratios in both cases indicate an increase trend as the ambient dry bulb temperature increases, which means that the higher the ambient temperature is, the more difficult it is to decrease the condensing temperature. And this observation transmits that the increase of dry bulb temperature could not only greatly increase the condensing temperature but also increase the difficulty in the effort of decreasing it by improvements. And in case 2, the condensing temperature decreases much more obviously than case 1, comparing to the default case.

Table 13 The condensing temperature increase ratio of two cases

| $T_d$ ,°C / Ratio of $T_c$ | 0 | 5 | 10 | 15 | 20 | 25 | 30 | 35 | 40 |
|---|---|---|---|---|---|---|---|---|---|
| $T_{c,1}/T_{c,D}$ | 0.871 | 0.883 | 0.892 | 0.900 | 0.907 | 0.913 | 0.918 | 0.922 | 0.926 |
| $T_{c,2}/T_{c,D}$ | 0.610 | 0.646 | 0.676 | 0.701 | 0.722 | 0.741 | 0.756 | 0.770 | 0.783 |

Similarly, Table 14 shows the ratio of the condensing pressure of case 1 and case 2 with respect to the default case. For both cases, it shows a similar increase in the condensing pressure ratio as the ambient dry bulb temperature increases. The condensing pressure in case 2 also shows more of a decrease than that of case 1.

Table 14 The condensing pressure increase ratio of two cases

| $T_d$ ,°C / Ratio of $P_c$ | 0 | 5 | 10 | 15 | 20 | 25 | 30 | 35 | 40 |
|---|---|---|---|---|---|---|---|---|---|
| $P_{c,1}/P_{c,D}$ | 0.727 | 0.733 | 0.739 | 0.745 | 0.751 | 0.756 | 0.761 | 0.766 | 0.771 |
| $P_{c,2}/P_{c,D}$ | 0.364 | 0.375 | 0.387 | 0.398 | 0.409 | 0.420 | 0.431 | 0.441 | 0.452 |

Table 15 The Rankine cycle efficiency increase ratio

| $T_d$ ,°C / Ratio of $\eta$ | 0 | 5 | 10 | 15 | 20 | 25 | 30 | 35 | 40 |
|---|---|---|---|---|---|---|---|---|---|
| $\eta_{c,1}/\eta_{c,D}$ | 1.033 | 1.034 | 1.035 | 1.037 | 1.039 | 1.041 | 1.043 | 1.045 | 1.047 |
| $\eta_{c,2}/\eta_{c,D}$ | 1.101 | 1.105 | 1.109 | 1.113 | 1.118 | 1.123 | 1.128 | 1.134 | 1.141 |

Table 15 shows the increasing ratio of the Rankine cycle efficiency of the two cases compared to the default one. It indicates an increasing trend in the ratio for both cases with respect to the default one, as the ambient dry bulb temperature increases. Moreover, for case 2 where the heat transfer surface area of the ACC was doubled, the Rankine cycle efficiency increased more than twice as that for case 1 with respect to the default case.

## Conclusion

An advanced circular-tube –circular-fin surface was applied and simulated. The results showed that it could improve the performance of the air-cooled condenser to some extent, which in turn enhanced the Rankine cycle efficiency. And a further doubled heat transfer surface area resulted in a more apparent improvement in the performance of the ACC as well as in the Rankine cycle efficiency. But the degree of the improvement was still affected by the increasing dry bulb temperature. An advanced surface of a different geometry other than the circular-tube-circular-fin might show benefits.

# CHAPTER 6

# A FLATTENED-TUBE SURFACE STUDY

## Flattened-Tube Surface

As the new circular-tube surface cases indicated, doubled heat transfer surface area resulted in a more apparent improvement in the performance of the ACC, a more new type of surface which could provide more heat transfer surface area will be explored in this chapter.

As one of the highly compact surfaces, the flattened-tube surface has been widely used to enhance the heat transfer, in which tubes are flattened so as to increase surface area that contacts the fins, as shown in Figure 26.

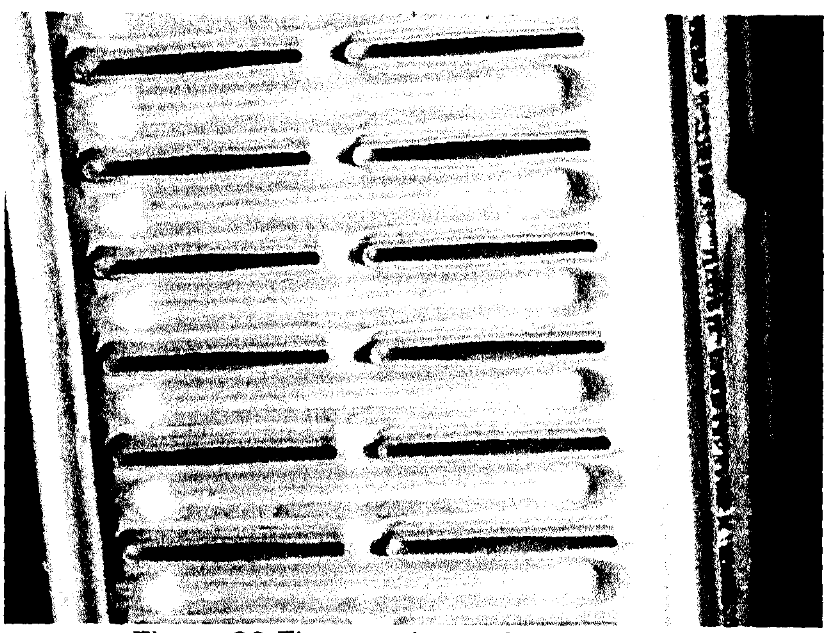

Figure 26 Flatten-tube surface structure

In this case, a flattened-tube surface with the highest $St * \Pr^{2/3}$ value was selected from the heat transfer surface pool provided by Kays and London. It will have the same number of rows and tubes per row as the default circular-tube surface will be applied to the air-cooled condenser. A similar Rankine cycle model will be simulated in GateCycle and compared to the default case as the previous new surface cases did.

## Equivalent Surface Conversion

In GateCycle, all the geometry inputs are for circular-tube surface, but none of them seems suited for other shape of tubes. When the geometry information for other tube configurations is entered, certain criteria are not met and the code issues warnings as it tries to find geometrically feasible inputs. As a result of this, to apply the flattened-tube surface to the ACC requires fooling GateCycle by entering round tube and fin geometry data that results in the same bare tube and total (bare tube + fin) surface areas provided by the non-round tubes and fins, as suggested by the GateCycle manual.

The most important geometry parameters that require conversions are outer tube diameter, hydraulic diameter of the tube and fin dimensions. The outer tube diameter and the fin dimensions together with some other variables, such as fin cover percentage, etc, will determine the total heat transfer area for the ACC. The hydraulic diameter of the tube will determine the Reynolds number of the air that is going through the surface, which further determines the heat transfer coefficient of this surface. Thus equivalent geometry and heat transfer characteristics of the flattened tube are converted to the circular tube.

Table 16 Geometry parameters of the flattened-tube surface conversion

| Geometry parameters | Flattened-tube | Geometry parameters | Equivalent circular-tube |
|---|---|---|---|
| Width of the tube (mm) | 18.72 | Tube outer diameter (mm) | 13.54 |
| Height of the tube(mm) | 2.54 | Hydraulic outer diameter (mm) | 8.45 |
| Gauge (mm) | 1.27 | Gauge (mm) | 1.27 |
| Pitch/outer diameter (normal to flow) | 13.97/equivalent diameter | Pitch/outer diameter (normal to flow) | 1.03 |
| Pitch/outer diameter (in the flow) | 1.3462/equivalent diameter | Pitch/outer diameter (in the flow) | 0.1 |
| Fin width (mm) | 83.82 | Fin width (mm) | 83.82 |
| Fin length (mm) | 145 | Fin length (mm) | 145 |
| Fin thickness (mm) | 0.305 | Fin thickness (mm) | 0.305 |
| Fin pitch (mm) | 2.73 | Fin pitch (mm) | 2.73 |

A flattened-tube surface with connected fins was selected and converted into the equivalent circular-tube surface as shown in the Table 16. As mentioned above, the number of rows and the number of tubes per row were kept the same as the default one, which are 3 rows and 40 tubes per row.

The parametric design of the Rankine cycle is shown in Table 17. As was done in the previous new surface case, most parameters were set the same as the default model for the flattened-tube case. An exception was that the condensing temperature was lowered to 31.39 °C, compared to 48.11°C for the default conventional dry cooling case, and the condensing pressure was accordingly brought down to 4.59 kPa, compared to 11 kPa for the default case. Also this surface provided more than twice surface area as the default one did.

Table 17 The parameters set up of the Rankine cycle for the flattened-tube case

| Rankine Cycle Parameters | Value |
|---|---|
| Mass flow rate of steam | 1 kg/s |
| Boiler pressure | 2300 kPa |
| Condensing pressure at the design mode | 4.59 kPa |
| Boiler efficiency | 90% |
| The steam quality at the turbine outlet | 0.8 |
| The steam quality at the boiler outlet | 0 |
| The steam quality at the air-cooled condenser outlet | 1 |
| Condensing temperature at the design mode | 31.39 °C |

Results and Discussions

Similar tests of the Rankine cycle with the new dry cooling system with double heat transfer surface area were run under various ambient dry bulb temperatures. Comparisons of the results were made between the flattened-tube case and the default case in Figure 27, Figure 28 and Figure 29.

Figure 27 compares the condensing temperature between the flattened-tube case and the default case. Both cases show a similar increasing trend of the condensing temperature as the ambient temperature increases, but the flattened-tube case shows an apparently lower condensing temperature. It reaches a condensing temperature of 72.98 °C, which decreases 19.49% compared to 90.65 °C in the default case, when the ambient temperature reaches 40 °C. And the condensing temperature of the flattened-tube case decreases about 25.9% on average compared to the default case.

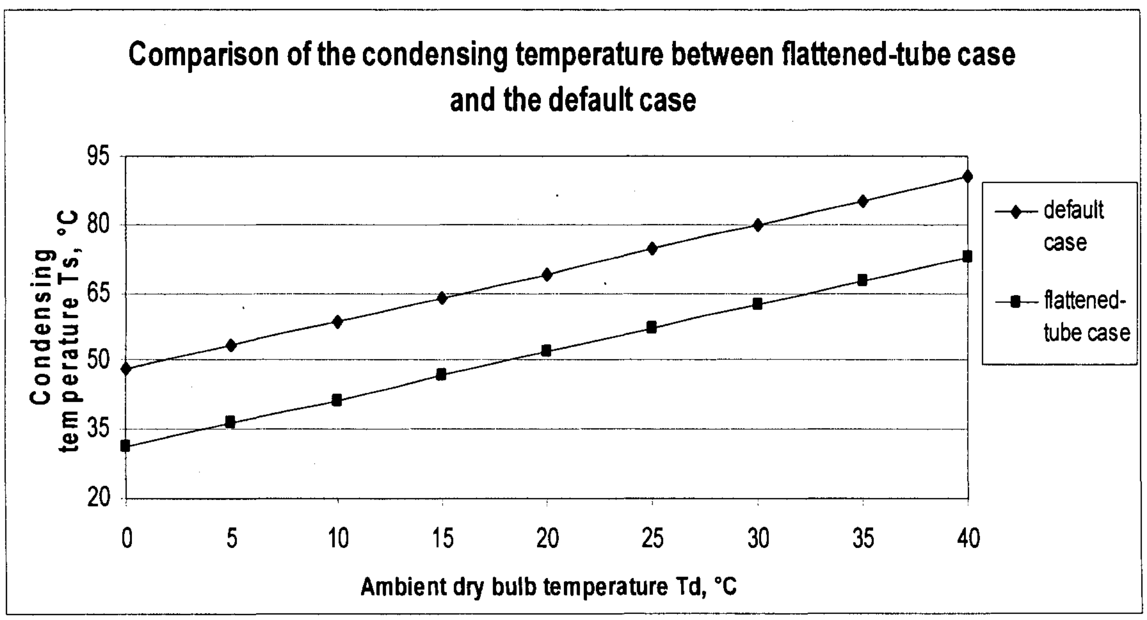


Figure 27 Comparison of the condensing temperature between the flattened-tube case and the default case

Figure 28 shows an increasing trend of the condensing pressure in both cases. However, it can be seen that the condensing pressure in the flattened-tube case increases much more slowly than the default case. It also shows an obviously lower condensing pressure of the flattened-tube case compared to the default case under all ambient temperatures. The condensing pressure in the flattened-tube case lowers 54.8% on average compared to the default case.

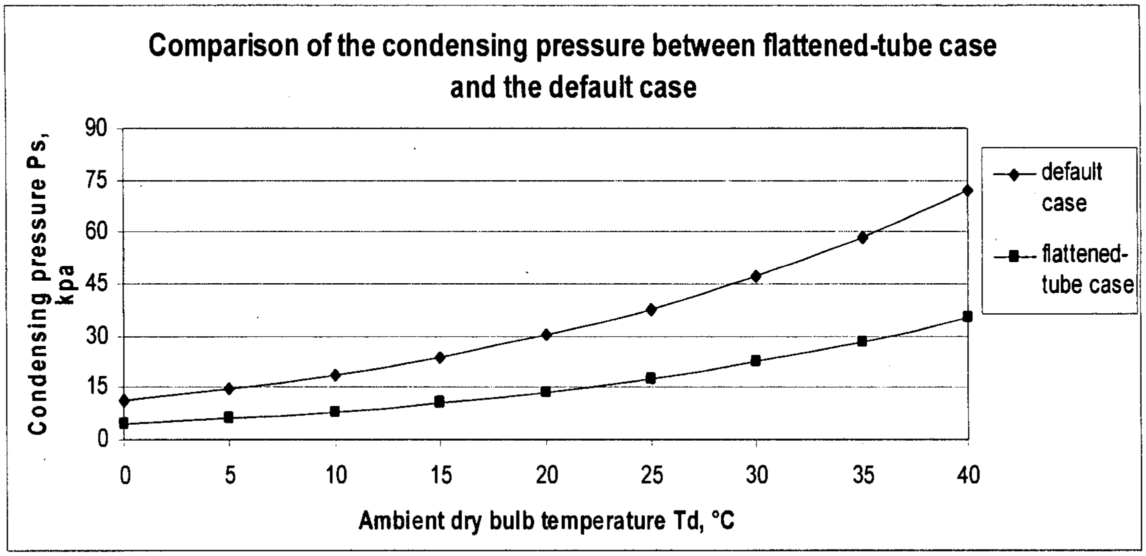


Figure 28 Comparison of the condensing pressure between the flattened-tube case and the default case

Figure 29 compares the Rankine cycle efficiency of the flattened-tube case and the default case. It also shows a linearly decreasing trend in the flattened-tube case, as the ambient dry bulb temperature increases. However, there is an average of 10.9% obvious increase of the Rankine cycle efficiency in the flattened-tube case compared to the default case.

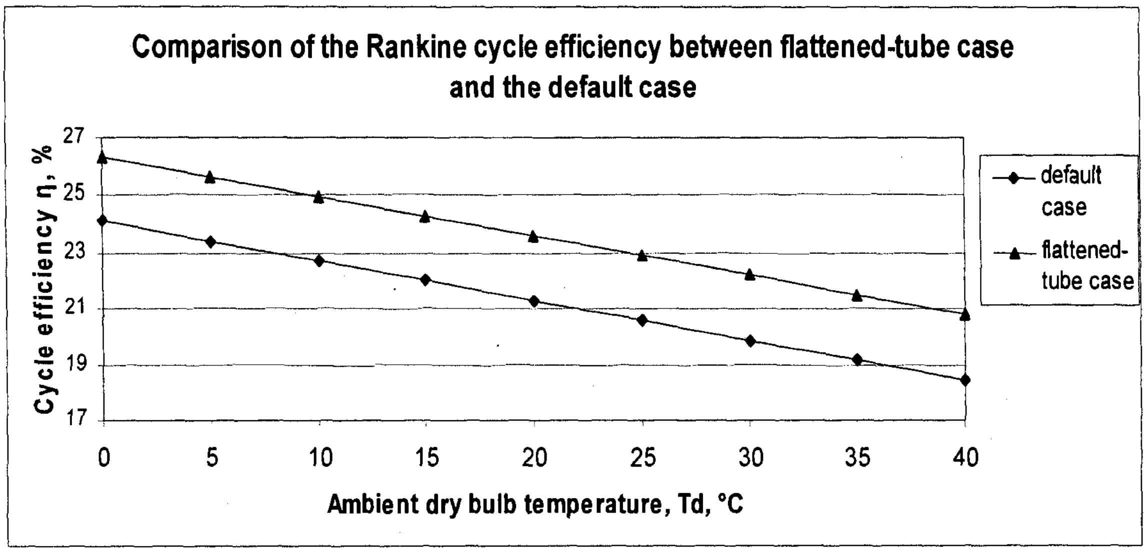


Figure 29 Comparison of the Rankine cycle efficiency between the flattened-tube case and the default case

## Conclusions

The flattened-tube surface could provide much more heat transfer surface area than circular-tube surface, and meanwhile occupies a smaller space. The simulation results proved that it apparently enhances the performance of the ACC and the Rankine cycle efficiency due to its high compactness. Such a surface could be a better option than the default one.

# CHAPTER 7

# CONCLUSIONS

In order to study the performance feature of the power plant with dry cooling systems under different ambient conditions, a power plant model with a conventional dry cooling system was modeled in GateCycle under 0 °C, and simulated under different ambient dry bulb temperatures varying from 0 °C to 40 °C. Default configurations given by GateCycle were applied to all the equipment in the model. GateCycle performance was verified by a Matlab code. A wet cooling counterpart was then modeled in GateCycle keeping the design specifications the same as before except for the wet cooling system part. The wet cooling system also used default configurations and the ambient conditions used in the model were set to be 0 °C for dry bulb temperature and 10% for relative humidity. Similar tests were run for the wet cooling counterpart under using a variety of ambient dry bulb temperatures and relative humidities. For further comparisons, ideal cases were defined for each cooling system. This was done by assuming the condensing temperature equals to the dry bulb temperature for the dry cooling system and the wet bulb temperature for the wet cooling system. The efficiency variations under different ambient conditions as well as the yearly power generation which is calculated based on the TMY2 data were compared among the four cases.

The variations of the ACC condensing temperature, condensing pressure and the Rankine cycle efficiency were studied for the conventional dry cooling case as the ambient dry bulb temperature increased from 0 °C to 40 °C. For the wet cooling counterpart, the Rankine cycle efficiency was studied as the ambient dry bulb temperature increased from 0 °C to 40 °C and the relative humidity increased from 10% to 30%. For the ideal cases, the resulting Rankine cycle efficiencies for the same ambient condition ranges were studied separately, and the yearly energy generations were calculated for each of the four cases using the TMY2 hourly data as well.

Comparing the results of the four cases, it is concluded that:

1. The condensing temperature and pressure of the conventional dry cooling system tends to increase as the ambient temperature increases, and the Rankine cycle efficiency tends to decrease at the same time.

2. The conventional dry cooling model is always less efficient than its conventional wet cooling counterpart, even if the conventional wet cooling counterpart is at the lowest cycle efficiency when the relative humidity reaches the highest value of all the tests. This is especially obvious when the ambient dry bulb temperature is high.

3. The ideal cooling systems always outperform the conventional ones under any ambient conditions.

4. The Rankine cycle efficiency of the ideal dry cooling system model was very close to the ideal wet cooling counterpart, which indicated the possibility that

the conventional dry cooling system may perform as well as the wet cooling system, if some potential improvements might apply.

An advanced circular-tube-circular-fin surface was selected from a pool of compact surfaces, and it was applied to the air-cooled condenser analysis. Similar simulations were carried out for the system with the new surface in two cases – equal surface area case and double surface area case. Results indicated a small but definite enhancement on the Rankine cycle efficiency for the first case, and a more obvious enhancement for the second one.

This advanced surface seems not a very realistic option to greatly improve the whole Rankine cycle performance, so a flattened-tube surface was explored due to its compactness.

It showed an obvious improvement on the performance of the ACC and the Rankine cycle efficiency compared to the default case, and thus turned out to be a good option for the ACC.

## APPENDIX

### Distribution of dry cooling units in the US

Table 18 Distribution of dry cooling units in the US [Layton and O'Hagan. 2002]

| State | Dry Cooling | | Hybrid, Wet/Dry | |
|---|---|---|---|---|
| | Number of Units | Capacity (MWe) | Water Conservation | Plume Abatement |
| Alaska | 2 | 75 | | |
| California | 6 | 273 | | 1 |
| Colorado | | | | 1 |
| Connecticut | 2 | 280 | | |
| Hawaii | 1 | 20 | | |
| Iowa | 1 | 40 | | 2 |
| Idaho | 1 | 40 | | 2 |
| Illinois | 1 | 9 | | 1 |
| Massachusetts | 8 | 454 | | |
| Maine | 2 | 100 | | |
| Michigan | 1 | 9 | | |
| Minnesota | 1 | 6 | | |
| Montana | 1 | 50 | | |
| New Jersey | 2 | 385 | | |
| New Mexico | | | 1 (660 MWe) | |
| Nevada | 1 | 150 | | |
| New York | 6 | 205 | | 2 |
| Pennsylvania | 2 | 88 | | 2 |
| Rhode Island | 1 | 80 | | |
| Texas | 2 | 450 | | 3 |
| Virginia | 2 | 100 | | 1 |
| Washington, DC | | | | 1 |
| West Virginia | 1 | 80 | | |
| Wyoming | 5 | 1180 | | |
| | | | | |
| Total US | 49 | 4074 | 1 (660 MWe) | 16 |

Matlab code

Below is the Matlab code for calculating the mass flow rate of the inlet air at the design mode and condensing temperature in the off-design mode.

```
% specified parameters for the problem

    Ms=1                    % Mass flow rate of the steam, kg/s
    Tain =0;                % Inlet air temperature in the design mode, °C
    d=0.021                 % Inner diameter of the ACC tube, m
    D=0.025                 % Outer diameter of the ACC tube, m
    Va=3.819                % Face velocity of the air, m/s

%in the design mode, the inlet air temperature is 0 °C, and the outlet air temperature is assumed to be 15 °C, so the air properties are obtained from the air property table at the mean temperature of 7.5 °C.

    Cp=1007                 % Specific heat of the inlet air, J/kg*K
    miu=14.6575x10^-6       % Kinematic viscosity  m^2/s
    Pr=0.7135               % Prandtl number of the air
    Ma=127.63               % Mass flow rate of the air kg/s
    C=0.36                  % Constant, 0.36 for 3 tube rows
    k=0.02535               % Thermal conductivity, W/m*K
    tfin=2.822              % Fin pitch, mm
    sfin=1.016              % Fin thickness, mm
```

hfin=20 % Fin height, mm

Re=Va*D/miu % Reynolds number of the air

% In the design mode, with the surface of the ACC selected as described above, the mass flow rate of the inlet air and the total heat transfer surface area is calculated as below.

$Nu=0.134*C*(Re^{0.681})*(Pr^{1/3})*((tfin\text{-}sfin)^{0.2})*((tfin\text{-}tfin)^{0.1134})/((hfin^{0.2})*(sfin^{0.1134}))$

h=Nu*k/D

% Assum the condensing temperature in the design mode

Ts =48

Hfg =XSteam('h_Tx',Ts ,0.8)-XSteam('h_Tx',Ts ,0)

% XSteam('h_Tx', Ts,0) is the enthalpy of the steam at the temperature of Tx and the quality of 0, similar for XSteam('h_Tx', Ts,0.8). Here the inlet steam quality is assumed to be 0.8.

epsilon= Ms*Hfg*1000/( Ma*Cp*(Ts-Tain))

NTU=-log(1-epsilon)

% Since the convective coefficient of the steam side is much higher than the air side, the overall heat transfer coefficient is approximately equal to the h value of the air side.

```
U=h
A=NTU*Cp*Ma/U
```

% In the off-designed mode, the ambient dry bulb temperature increases to 15 °C, and the according condensing temperature is calculated.

```
Tain1=15
Ts2 =60   % Condensing temperature is assumed first, and trial and error method is used to find out its true value.
Ts1 =62
difference = Ts1 -Ts2
adiff = abs(difference)
while adiff >1
    Ts2 =Ts1
    Hfg =XSteam('h_Tx',Ts2 ,0.8)-XSteam('h_Tx',Ts2 ,0)
    Qmax=Ms*Hfg/epsilon
    Ts1=Qmax*1000/(Ma*Cp)+Tain1
    difference = Ts1-Ts2
    adiff = abs(difference)
```

```
end

%for point 1, T1, p1 and X1 are known, h1 and s1 are to be found.
    T1=220 % the boiler temperature
    p1=23% the boiler pressure, bar
    h1=XSteam('h_pT',p1,T1) %kJ/kg
    s1=XSteam('s_pT',p1,T1)

%For point 2,
    T2=Ts1
    p2=XSteam('psat_T',T2)
    X2=0.8
    h2=XSteam('h_px',p2,X2)
% the actual turbine output is calculated by
    Wact=Ms*(h1-h2) % kW

% For point 3, p3 and s3 are to be found.
    p3=p2
    T3=T2
    h3=XSteam('hL_p',p3)
    s3=XSteam('sL_T',Ts1)
% The work consumed by the pump is calculated by
    s4=s3
```

```
v3=XSteam('vL_p',p3) %m^3/kg

v4=XSteam('v_ps',p1,s4)

vm=0.5*(v3+v4)

Wp=vm*Ms*(p1-p3)*100 %kW


%For point 4, h4 is to be found.

p4=p1

T4=XSteam('T_ps',p4,s4)

h4=XSteam('h_ps',p4,s4)

%Heat consumed by the Rankine cycle is calculated by

Qin=Ms*(h1-h4)/0.9

%Rankine cycle efficiency is calculated by

eff=(Wact-Wp)/Qin
```

Parameters configuration for the conventional dry and wet cases

Figure 30, Figure 31, Figure 32 and Table 19 show the parameters set up for the air-cooled condenser in Chapter 3.

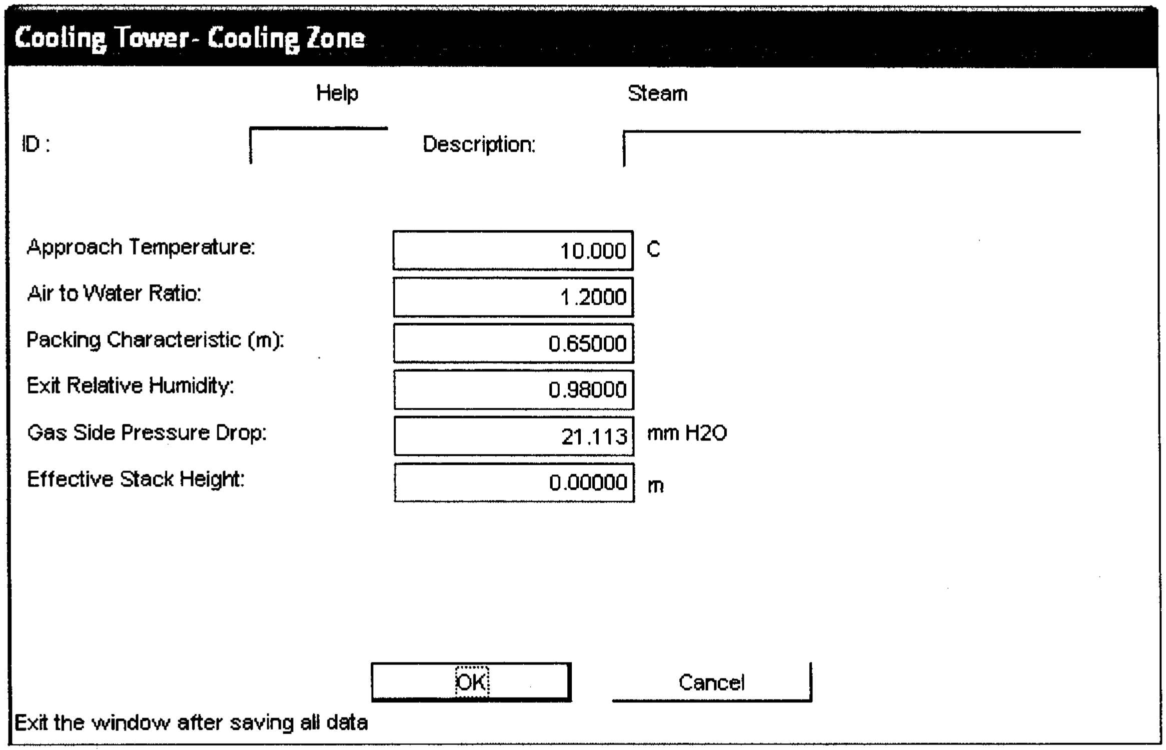

Figure 33 Cooling zone parameters set up for the wet cooling tower

**Table 19**

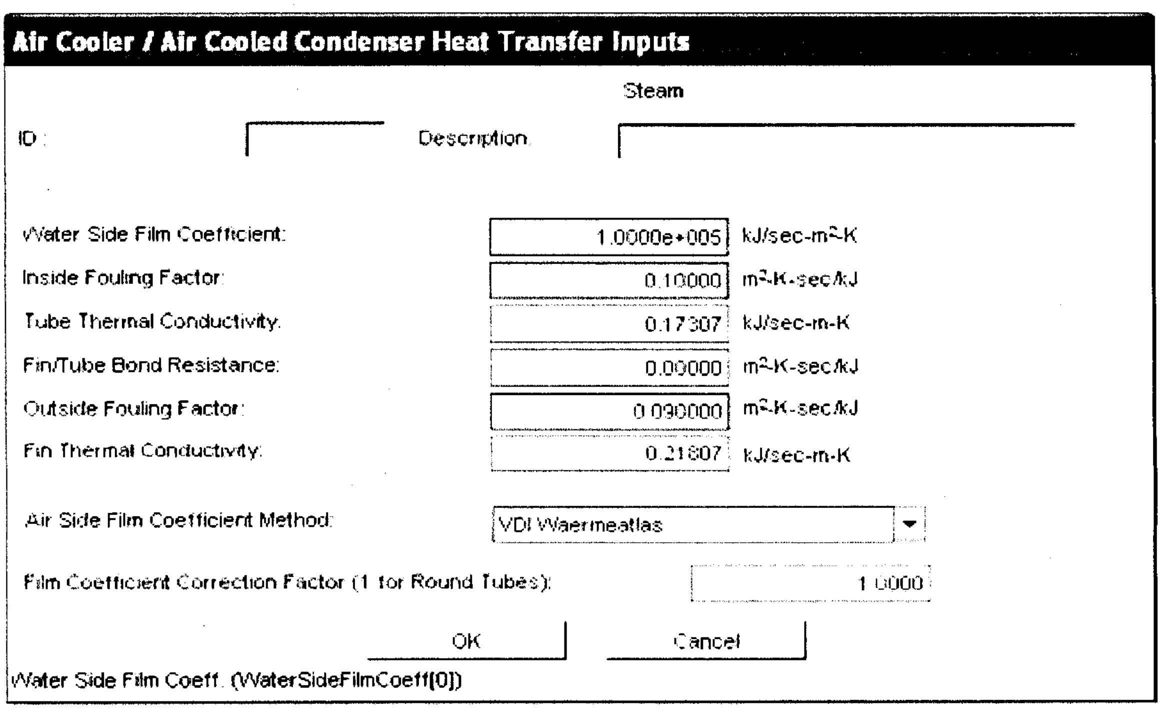

Figure 30 Heat transfer parameters set up for the air-cooled condenser

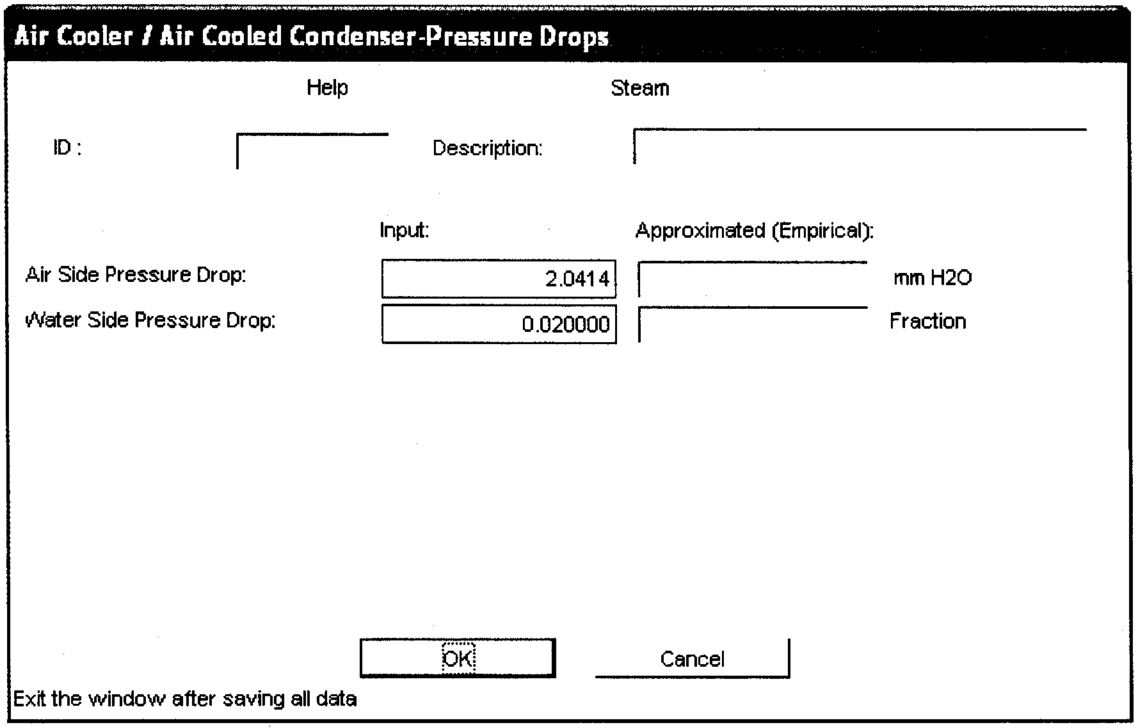


Figure 31 Pressure drop parameters set up for the air-cooled condenser

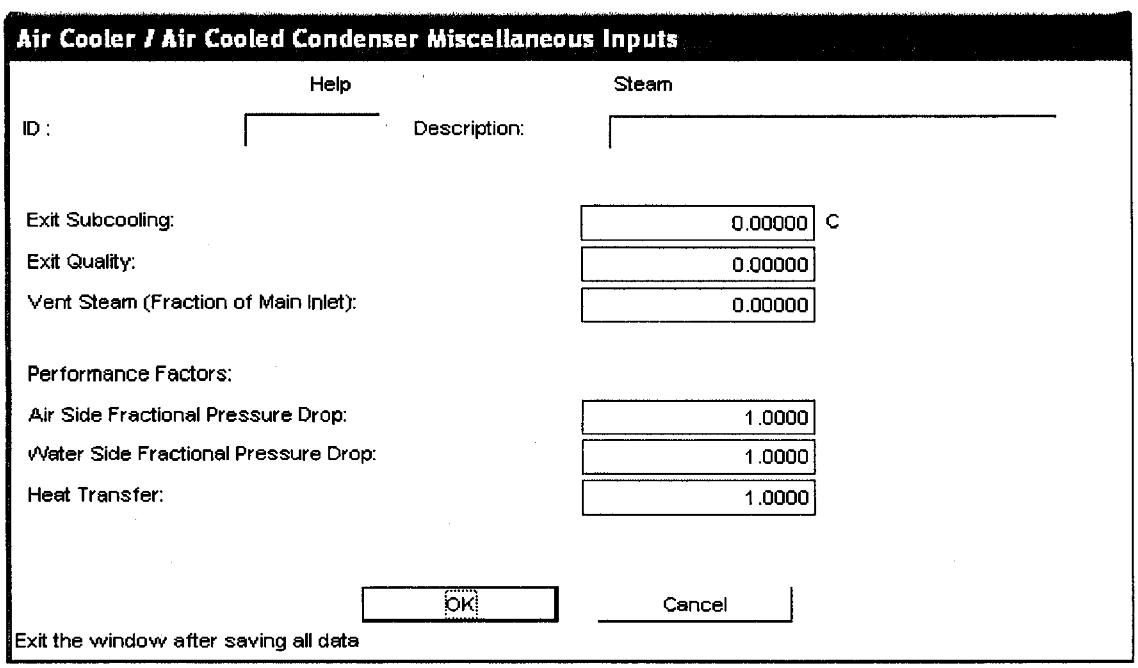

Figure 32 Miscellaneous parameters set up for the air-cooled condenser

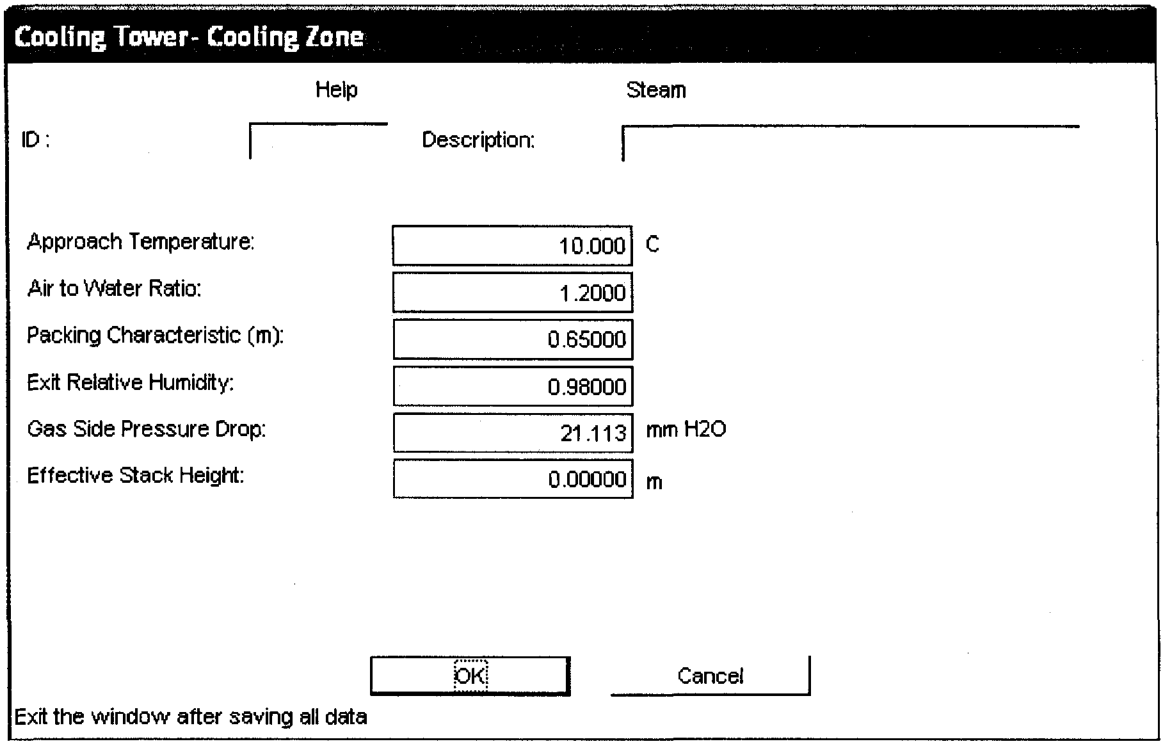


Figure 33 Cooling zone parameters set up for the wet cooling tower

Table 19 Geometry parameters set up for the air-cooled condenser

| ACC Parameters | Values |
|---|---|
| inlet air temperature at the design mode, | 0 |
| Mass flow rate of air | 131.70kg/s |
| Total heat transfer surface area of ACC | 816.39 m^2 |
| Velocity of inlet air | 3.5 m/s |
| Length of ACC tubes | 5 m |
| Number of tubes per row | 19 |
| Number of rows | 3 |

| | |
|---|---|
| Outer diameter of the tubes | 25.4 mm |
| Inner diameter of the tubes | 22.86 mm |
| Diameter of the fin | 40 mm |
| Thickness of the fin | 1.016 mm |
| Pitch of the fin | 2.822 mm |

Figure 33, Figure 34 and Figure 35 show the parameters set up for the wet cooling tower.

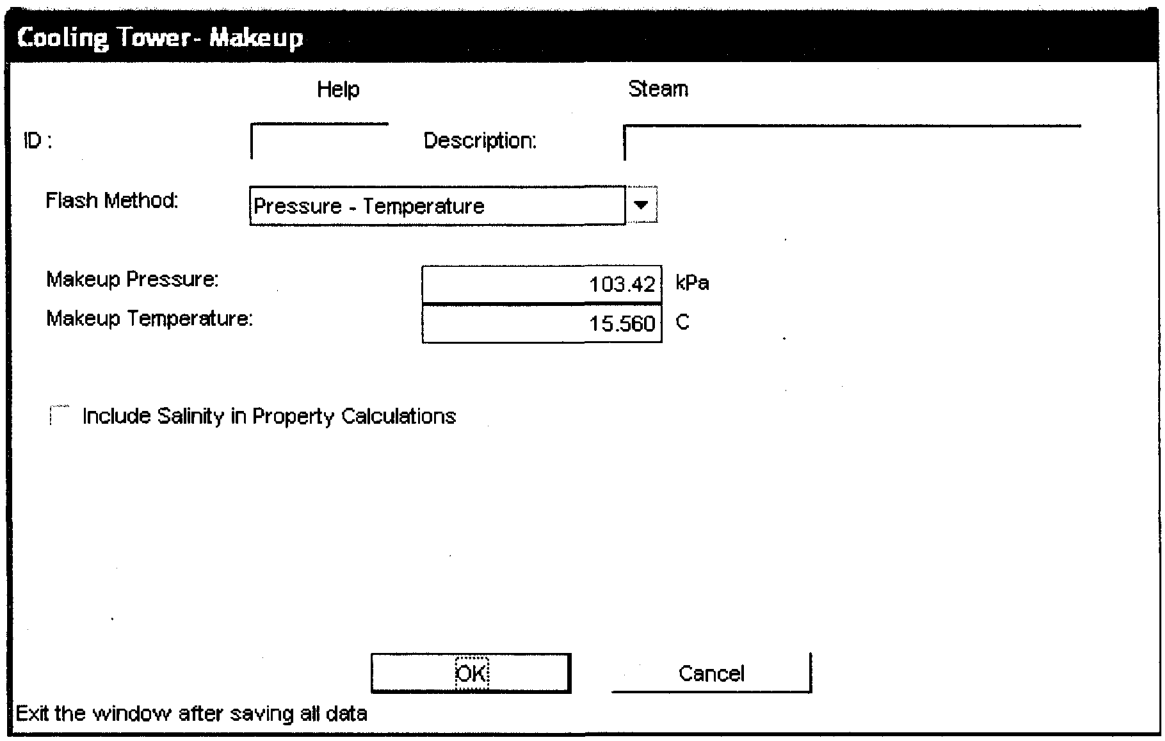


Figure 34 Makeup parameters set up for the wet cooling tower

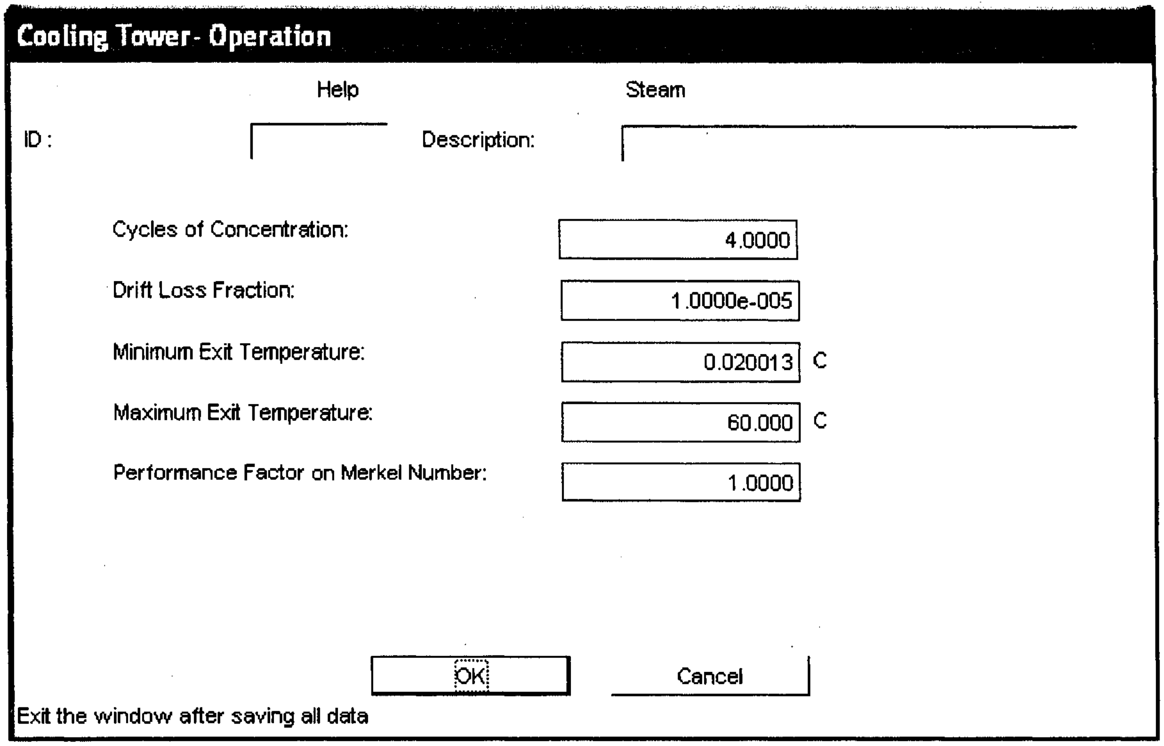


Figure 35 Operation parameters set up for the wet cooling tower

## REFERENCES


Azad, E. and Karimeddini, Z.K. 1986. New Concept of Heat-pipe Cooling for Thermal Power Plant in High Ambient Temperatures. *Journal of the Institute of Energy*, v 63, n 456, p 119-123

Backer, L. D and Wurtz William M. 2003. Why Every Air Cooled Condenser Needs A Cooling Tower. Paper No.: TP03-01, Presented at the Cooling Technology Institute Annual Conference, San Antonio, Texas.

Bartz, John A. 1988. Dry Cooling of Power Plants - A Mature Technology? *Power Engineering*, v 92, n 10, p 25-27

Conradie, T.A. and Kroger, D.G. 1991. Enhanced Performance of a Dry-cooled Power Plant through Air Precooling. Proceedings of the International Power Generation Conference, San Diego, CA, p 1-6.

Electric Power Research Institute, 1986. Advanced Dry-cooling Demonstration: Summary. Electric Power Research Institute, Coal Combustion Systems Division, (Report) EPRI CS, Dec, 60p

Hintzen, F.J. and Benzing, W. 1999. Increased Use of Dry Cooling in International Power Station Projects. *VGB PowerTech*, v 79, n 10, 4p

Larinoff M.W., Moles, W.E. and Reichhelm, R. 1978. Design and Specification of Air-Cooled Steam Condensers. Reprint from Chemical Engineering, Hudson Products Corporation Houston, Texas

Layton, Matthew S. and O'Hagan, Joseph. 2002. Comparison of Alternate Cooling Technologies for California Power Plants. California energy commission.

Johnson, B. M. and Maulbetsch, J S. 1979. Dry Cooling for Power Plants: Incentives, Problems, and R&D Activities. Proceedings - Annual Offshore Technology Conference, v, n 2, p 747-769

Kays, W. and London, A. L.. 1998. Compact Heat Exchangers. Krieger Publishing Company, Malabar, Florida.

Khalil, Ibrahim, 2006. Performance of Plate Fin Compact Heat Exchangers. MSME Thesis, UNLV.

Kroeger, D. G. 1998. Air-cooled Heat Exchangers and Cooling Towers. New York: Begell House.

Larinoff, M. W. and Forster, L. L. 1977. Dry and Wet-peaking Tower Cooling Systems for Power Plant Application. American Society of Mechanical Engineers, Paper 77-WA/Pwr-2, 12p

Leung, Paul. 1973. Dry Cooling Tower Plant Operation: an Economic Loading Approach. Conference: ASME Winter Annual Meeting, Heat Transfer Division Symposium, Nov 11-15, Detroit, p 77-83.

McHale, Claire E. , Webster, David J., Jablonka, Glen E., Bartz, John A. 1979. New Developments in Dry Cooling of Power Plants. Proceedings of the American Power Conference, v 41, p 673-684.

Miliaris, E. S. 1974. Power Plants with Air-Cooled Condensing Systems. Cambridge, Massachusetts: The MIT Press.

Oplatka, G. 1981. Improved Operating Characteristic of Dry Cooling Towers by Partial Precooling of the Air. *Brown Boveri Review*, v 68, n 3-4, p 136-143.

Wyatt Enterprises, LLC. 2007.http://www.wyattllc.com/GateCycle/GateCycle.html

VITA
Graduate College
University of Nevada, Las Vegas

Deng, Huifang

Local Address:
4441 Escondido St. Apt 2206
Las Vegas, Nevada 89119

Degrees:
Bachelor of Science, Thermal Engineering, 2006
University of Science and Technology Beijing, China

Special Honors or Awards:
First Place of Campus Digital Video Contest, 2003
People Scholarship every year in college

Publications:

Deng, HF., Boehm, R. "An Estimation of The Performance Limits of Dry Cooling on Trough-Type Solar Thermal Plants". ASME Conference Proceedings (2008). (Submitted and accepted)

Thesis Title: An Estimation of the Performance Limits and Improvement of Dry Cooling On Trough Solar Thermal Plants.

Thesis Examination Committee:
Chairperson, Dr. Robert Boehm,
Committee Member, Dr. Yitong Chen,
Committee Member, Dr. Woosoon Yim,
Graduate Faculty Member, Dr. Yahia Baghzouz.